High Energy Neutrino Astrophysics– A. A. 2020-21

Lessons 3 and 4

- Measurement of the C.R. electromagnetic component: primary photons and electrons: how to detect photons and electrons ?
- Features, and experimental resolutions, of the devices used in the detectors in space: measurements of charge, mass, moment, energy, direction.
- Detection of primary cosmic rays with E <100 GeV.
- Main characteristics of apparatuses on atmospheric balloons and on space, main results.

Let's recall …

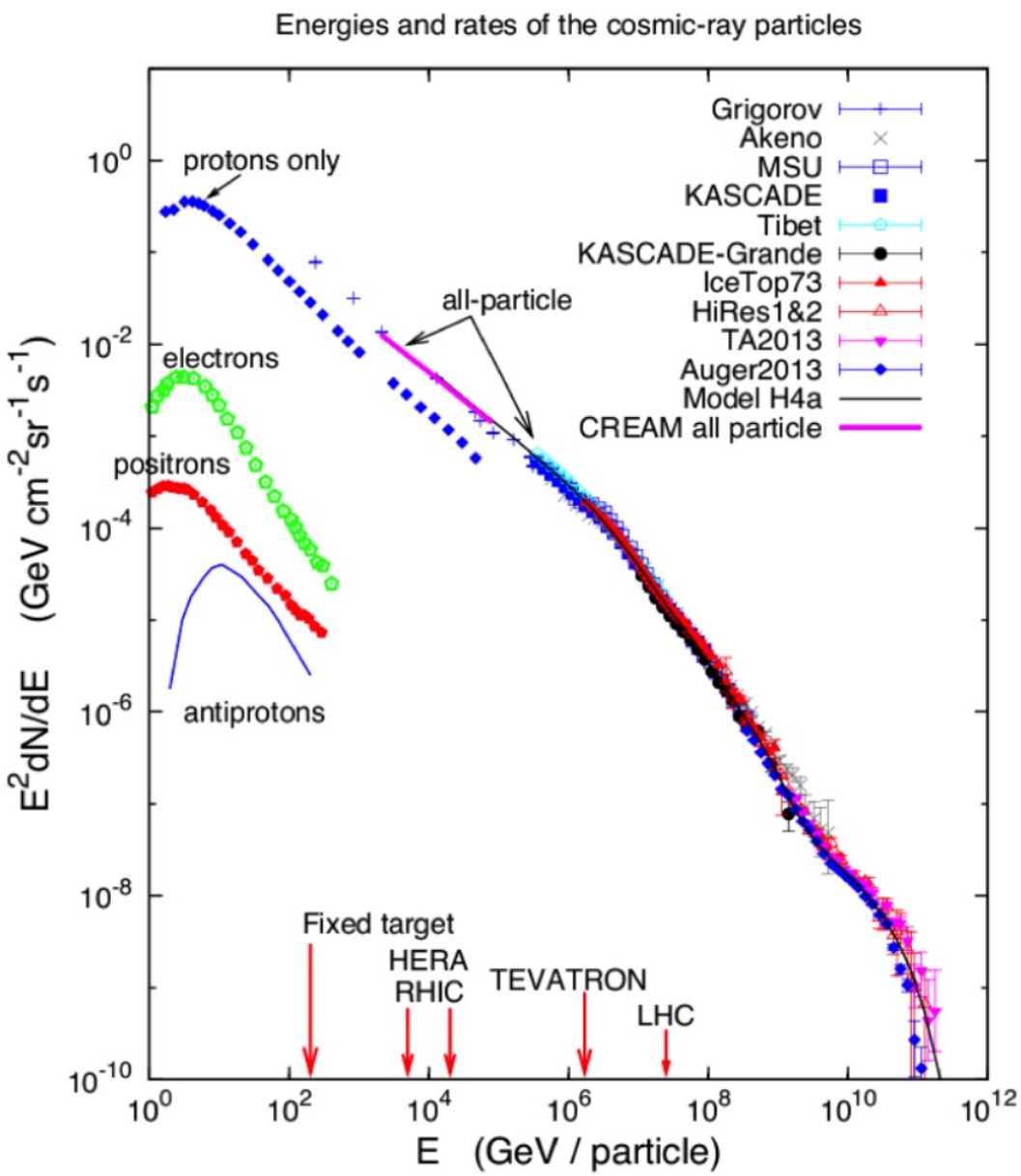
Energies and rates of the cosmic-ray particles
Grigorov
Akeno
MSU
KASCADE
Tibet
KASCADE-Grande
IceTop73
HiRes1&2
TA2013
Auger2013
Model H4a
CREAM all particle
protons only
all-particle
electrons
positrons
antiprotons
Fixed target
HERA
RHIC
TEVATRON
LHC
E²dN/dE (GeV cm⁻² sr⁻¹ s⁻¹)
E (GeV / particle)

Photons are also present in C.R.

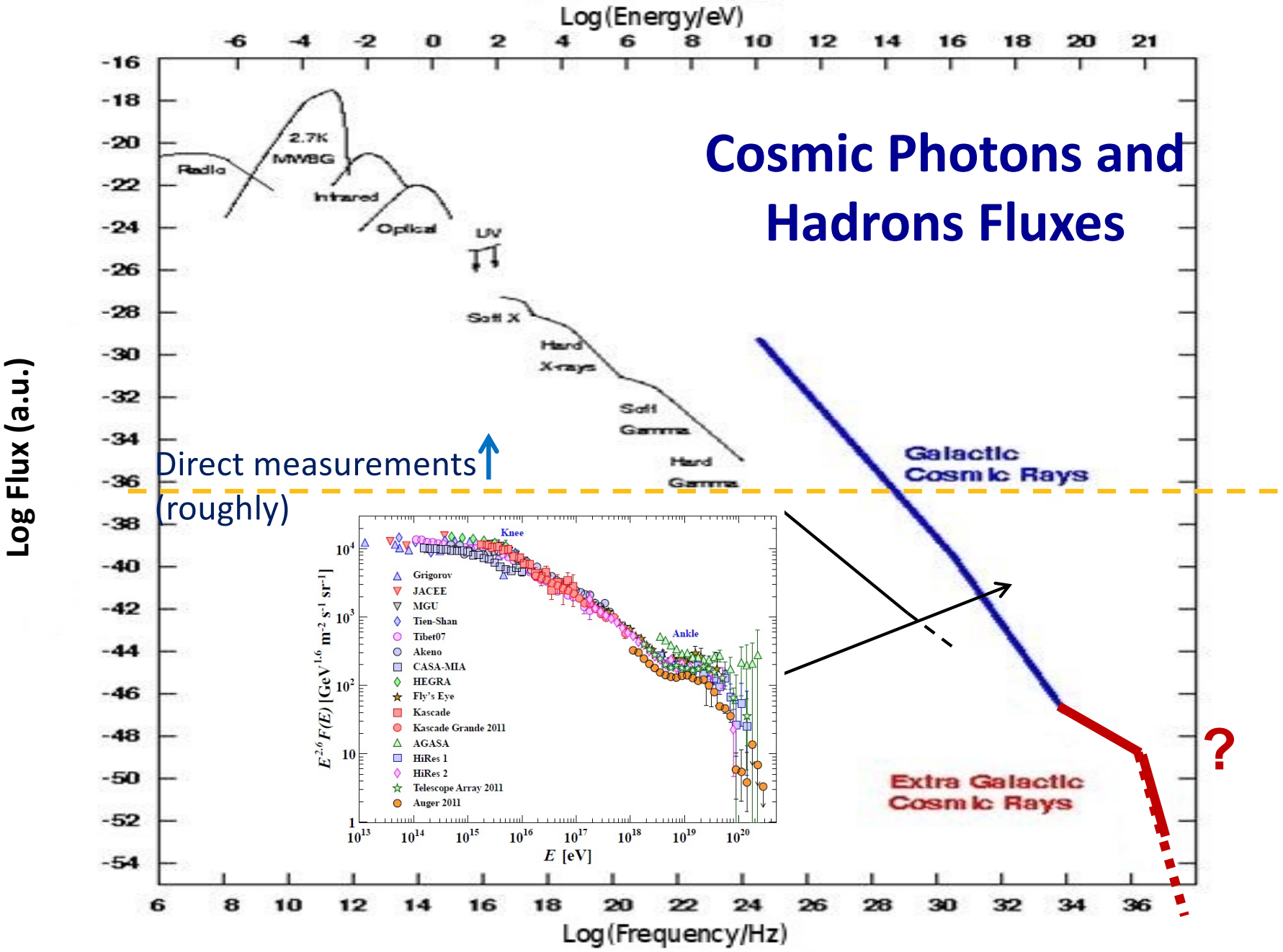

Astronomy with charged C.R. and with ”cosmic” photons

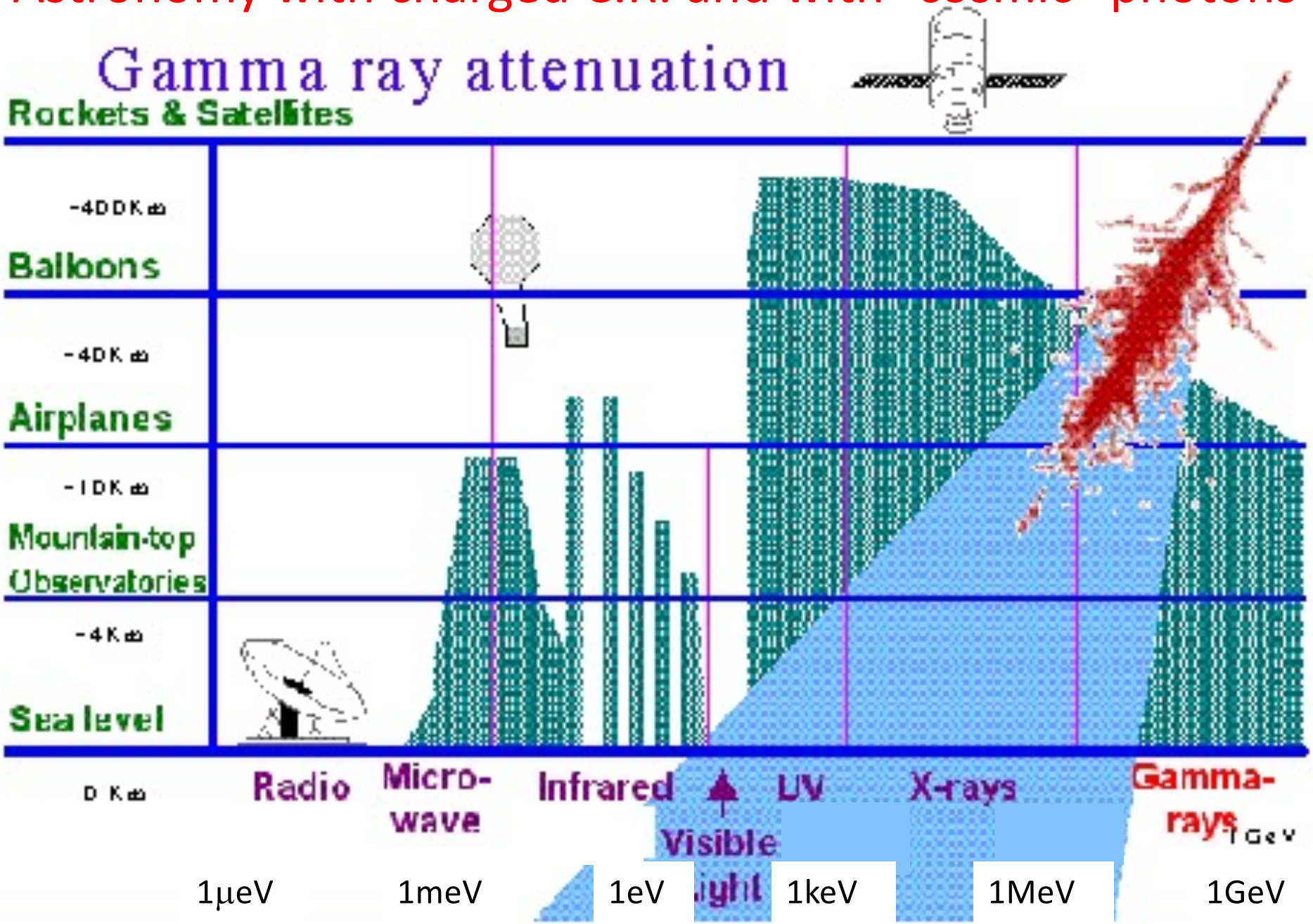

nomenclature used in astrophysics of C.R.s

Energy range	Name	Experimental Techniqu
10-30 MeV	Medium	Satellite
30Mev-30Gev	High Energy (HE)	Satellite
30 GeV - 30 TeV	Very High Energy (VHE)	Cerenkov Array (g.b.)
30 Tev - 30 PeV	Ultra High Energy (UHE)	Ground Based Array
30 Pev ->	Extremely High Energy (EHE)	Ground Based

Detection of charged C.R. and photons: preliminary considerations

The measurement of astrophysical photons on Earth possible for E_γ <1-10 GeV.

- The Earth's atmosphere corresponds to about 28 χ_0 (radiation lengths) and to about 11 λ_{int} (interaction lengths): it absorbs the HE photons. A direct measurement of 'primary' astrophysical photons above 100 GeV nearly impossible on the Earth.

- H.E. gamma rays from astrophysical sources could be detected outside the atmosphere but their flux is very faint and decreases significantly with energy: difficult to collect a good statistics in a reasonable time
  - For example: from "Vela", a "very active" gamma source with an integral γ flux

    $\Phi(E>100MeV)=1.3\times10^{-5}$ photons cm^{-2} s^{-1}

    with a detection area A$\simeq$ 1000 cm^2, in 1 minute: $N_{ev}=1.3\cdot10^{-5}$ x 1000 x 60 $\lesssim$ 1 event

    knowing that the energy spectrum is $dN/dE \propto E^{-1.89}$ we can calculate that to detect 1 photon with energy > 2GeV we should collect data for 2 hours

- The measurement of H.E. photons from astrophysical sources is difficult since the background (due to the flux of charged cosmic rays) is very high: the flux of charged cosmic rays is much more intense ($\sim$100) than the gamma one:

$$\frac{d\Phi}{dE} \cong 9\times10^{-6}\, E_{TeV}^{-2.76}\ \mathrm{cm^{-2}s^{-1}sr^{-1}TeV^{-1}}$$

Radiation length

- The radiation length (X_0 : the characteristic length that describes the energy decay of a beam of electrons:

$$X_0 = \frac{716.4 \text{ g cm}^{-2} A}{Z(Z+1)\ln(287/\sqrt{Z})}$$

- Distance over which the electron energy is reduced by a factor of 1/e due to radiation losses only
- Radiation loss is approx. independent of material when thickness expressed in terms of X_0
- Higher Z materials have shorter radiation length
  - want high-Z material for an EM calorimeter
  - want as little material as possible in front of calorimeter

material	X_0 g/cm^2
H_2	63
Al	24
Fe	13.8
Pb	6.3

- Example:
  lead: $\rho = 11.4$ g/cm^3 so $X_0 = 5.5$ mm

- The energy loss by brem is:

$$-\frac{dE}{dx} = \frac{E}{X_0}$$

Energy loss of photons and EM showers

- High-energy photons predominately lose energy in matter by e+e− pair production
- The mean free path for pair production by a high-energy photon

$$\lambda = \frac{9}{7} X_0$$

- **Note for electrons $\lambda = X_0$**

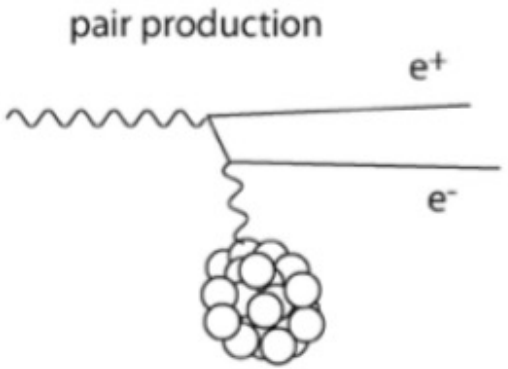

- But then we have high energy electrons…so the process repeats!
  - This is an electromagnetic shower!
  - An electromagnetic cascade as pair production and bremsstrahlung generate more electrons and photons with lower energy

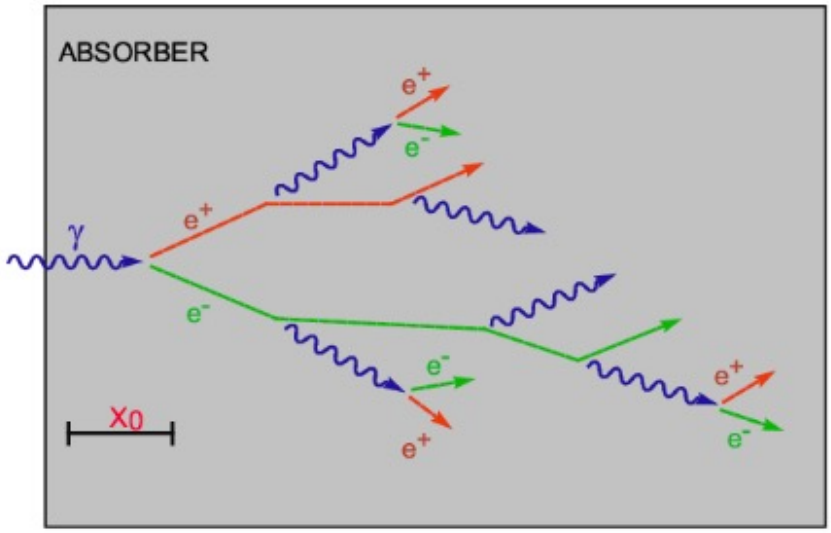

Energy loss of photons and EM showers

electrons

- *(bremsstrahlung)*

$$-\frac{dE}{dx} \propto \frac{Z^2 E}{m^2} \qquad \langle\theta\rangle \sim \frac{m_e c^2}{E_0}$$

$$-\frac{dE}{E} = \frac{dx}{X_0}$$

→ *Radiation length χ_0* : $X_0 \propto \frac{A}{Z^2}$

→ *Critical energy E_c*

$$\left(\frac{dE}{dx}\right)^{brem}_{E_c} = \left(\frac{dE}{dx}\right)^{ion}_{E_c}$$

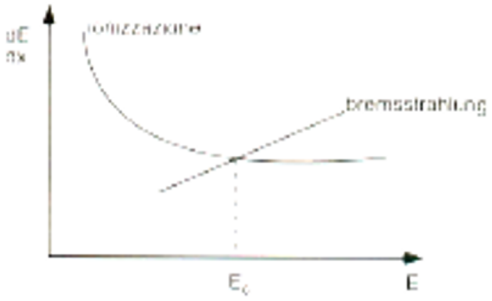

$$E_c \sim \frac{610 MeV}{Z + 1.24}$$ *(Solids, liquids)*

photons

- *Photoelectric effect*

$\sigma_{ph} \propto Z^5$

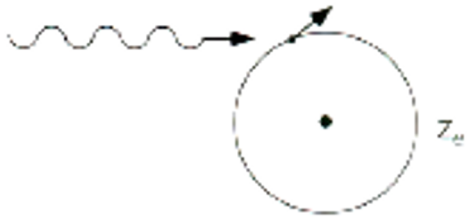

- *Compton diffusion*

$\gamma + e \rightarrow \gamma + e^-$

$$\sigma_c = Z \frac{\ell n \varepsilon}{\varepsilon} \qquad \varepsilon = \frac{E_\gamma}{m_e c^2}$$

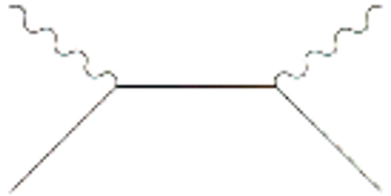

- *$e^+ e^-$ pair production*

$$\sigma_{pair} \approx \frac{7}{9} \frac{A}{N_A} \frac{1}{X_0}$$ (E_γ indip.)

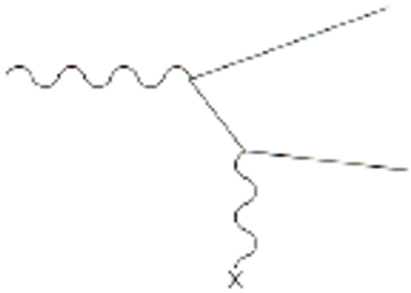

Energy loss of photons and EM showers

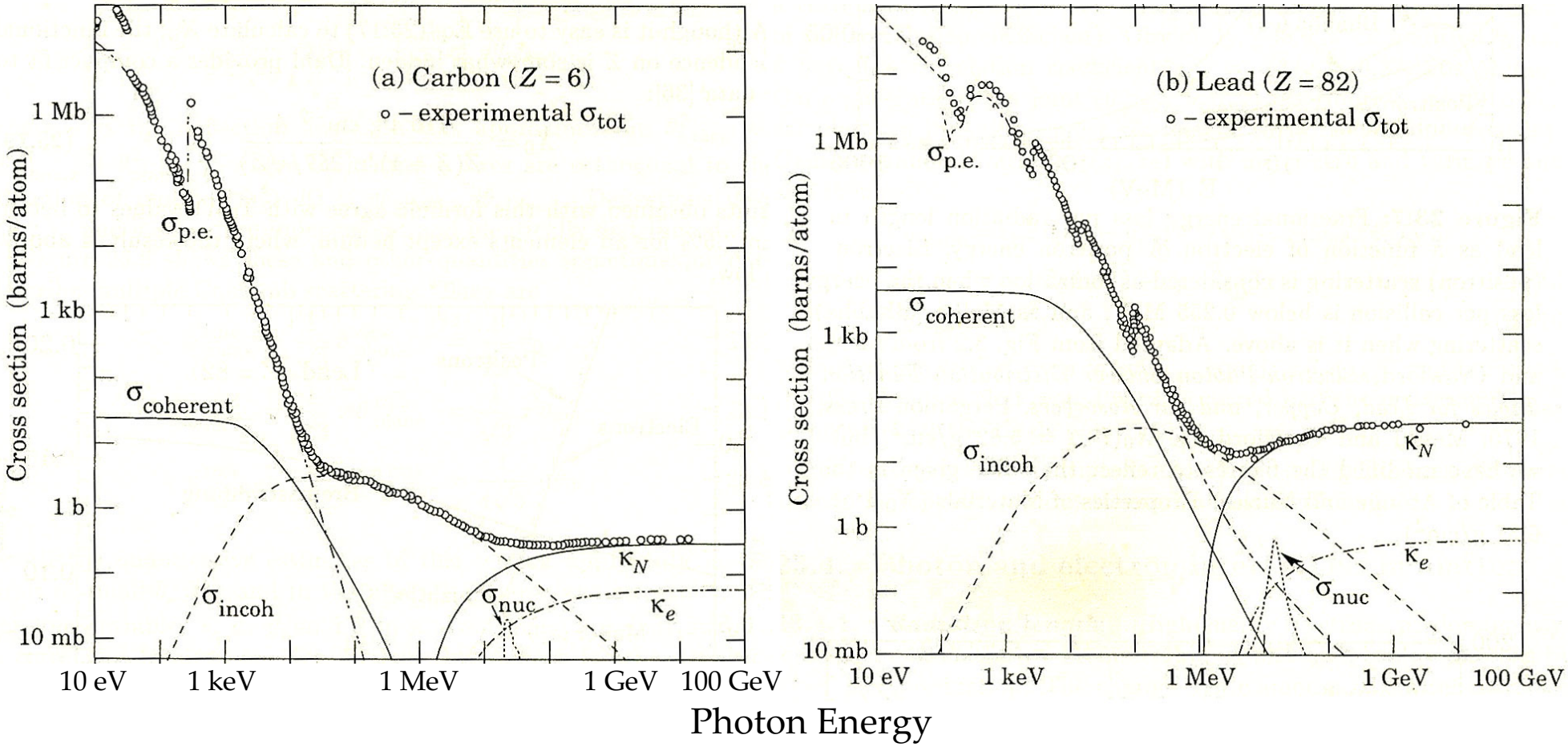

Total cross section for carbon and lead photons according to photon energy. The contributions of the different processes are shown:

$\sigma_{p.e.}$ = Atomic photoeffect (electron ejection, photon absorption)

$\sigma_{coherent}$ = Coherent scattering (Rayleigh scattering—atom neither ionized nor excited)

$\sigma_{incoherent}$ = Incoherent scattering (Compton scattering off an electron)

κ_n = Pair production, nuclear field

κ_e = Pair production, electron field

σ_{nuc} = Photonuclear absorption (nuclear absorption, usually followed by emission of a neutron or other particle)

Simplified scheme for an EM shower development: ”Toy Model” to describe an e.m. shower development

In each interaction:

- $e \rightarrow e'\gamma$
- $\gamma \rightarrow e^+e^-$ **(1)**

the number of particles doubles and the energy of each particles is ½ of the energy of the parent.

In each “step” t the N(t) increases and E(t) decreases:

$$N(0) = 1, \quad E(0) = E_0$$
$$N(1) = 2, \quad E(1) = \frac{E_0}{2}$$
$$N(2) = 4, \quad E(2) = \frac{E_0}{4}$$
$$N(3) = 8, \quad E(3) = \frac{E_0}{8}$$
$$N(t) = 2^t, \quad E(t) = \frac{E_0}{2^t}$$

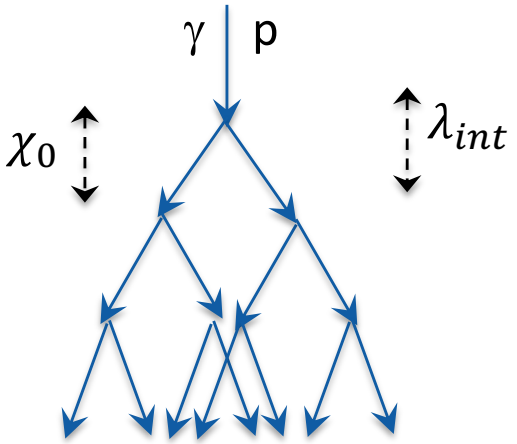

the multiplication of particles continue until the energy of electrons and gammas are sufficient to give the interactions **(1)** , i.e. until when the energy E(t)=$E_{critical}$. After that point the number of particles in the shower does not increase any more: the shower has reached the maximum development: we have: $N_{max} = N(t_{max})$ particles with energy $\boldsymbol{E(t_{max}) = \frac{E_0}{2^{t_{max}}} = E_{critical}}$ at a distance $\boldsymbol{X_{max} = \chi_0 \cdot t_{max}}$

We can then write the relation $\boldsymbol{t_{max} = \frac{1}{\ln(2)} \ln(\frac{E_0}{E_{critical}})}$

EM showers characteristics

- ***longitudinal distribution***

$$\frac{dE}{dt} \propto t^{\alpha} e^{-\beta t}$$

- ***Position of shower maximum***

$$t_{max} = 1.4 \ell n \frac{E_0}{E_c}$$

- ***Longitudinal containment***

$$t_{95\%} = t_{max} + 0.08Z + 9.6$$

- ***Lateral containment dominated by multiple scattering (+ photon propagation)***

$$\langle \theta_M \rangle = \frac{21}{p\beta} \sqrt{t}$$

$$r_{95\%} = 2R_M$$

$$R_M = \frac{21 MeV}{E_c} X_0 \quad g/cm^2$$ ***Molière radius***

$$R_M \propto \frac{X_0}{E_c} \propto \frac{A}{Z} \text{ per } Z >> 1$$

Interaction length and nuclear radiation length

Nuclear interaction length: is the mean path length required to reduce the numbers of relativistic charged particles by the factor 1/***e***, or 0.368, as they pass through matter.

- Interactions of heavy particles with nuclei can also produce hadronic showers
- Described by the **nuclear interaction length**

$$\lambda_n \approx 35\, g cm^{-2} A^{1/3}$$

- For heavy (high Z) materials we see that the nuclear interaction length is a lot longer than the electromagnetic one, $\lambda_n > X_0$
- So hadronic showers start later than electromagnetic showers and are more diffuse

- Example: lead ~ steel = 17 cm

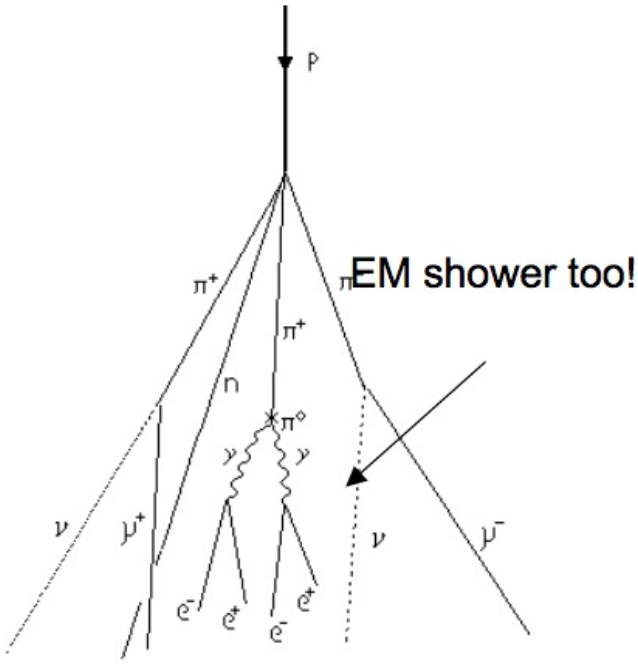

material	X_0 (g/cm^2)	λ_n (g/cm^2)
H_2	63	52.4
Al	24	106
Fe	13.8	132
Pb	6.3	193

Nuclear interaction length

- The interaction of energetic hadrons (charged or neutral) is determined by various nuclear processes:

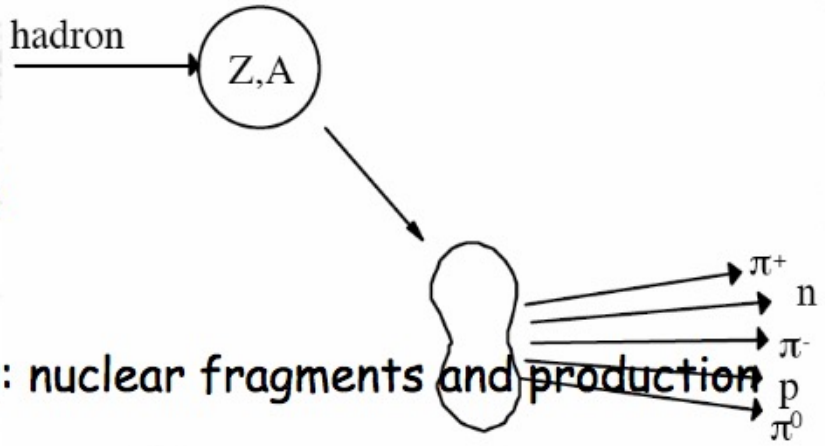

Multiplicity ∝ ln(E)

P_t < 1 GeV/c

- Excitation and finally breakup of nucleus: nuclear fragments and production of secondary particles
- For high energies (> 1GeV) the cross-sections depend only little on the energy and on the type of the incident particle (p, π, K, …)
- Define in analogy to X_0 a hadronic interaction length λ_I:

$$\lambda_I = \frac{A}{N_A \sigma_{total}} \propto A^{\frac{1}{3}}$$

Sources of astrophysical photons

All these radiations could be also "thermal", ie emitted by hot matter in equilibrium with the source temperature

Electromag. radiation	Typical production mechanism
Radio	Synchrotron Radiation due to GeV electrons spiralising into the source magnetic field. Typical source: Pulsar. This radiation has a continuous spectrum up to X
Infrared	Typically is a "reprocessed radiation". More energetic radiation interacting with the matter around the source (e, p, atoms) induces molecular rotational/vibrational transitions and loses energy
Optical	Emitted in transitions of atoms in excited states in Stars
Ultraviolet	Radiation emitted typically in Compton scattering (the low energy photon) in sources with production of high energy photons
X ray	Synchrotron Radiation due to TeV electrons spiralising into the source magnetic field. Typical source: Pulsar.
Gamma ray	High energy photons from sources where electron or proton are accelerated in shock waves.

Synchrotron Radiation

Synchrotron radiation is observed in regions where relativistic electrons spiral around magnetic field lines. This process results in strongly polarised radiation concentrated in the direction of the electrons motion (called "beaming"). Similar to bremsstrahlung, synchrotron has a characteristic shape of its spectra which is a power law spectrum. The shape of the spectrum produced is dependant on the energy distribution of the emitting electrons and is easily distinguishable from thermal blackbody radiation.

The characteristic photon energy is $\varepsilon_{\gamma,s}=h\omega_B\gamma^2/2\pi= heB\gamma^2/(2\pi mc)$.

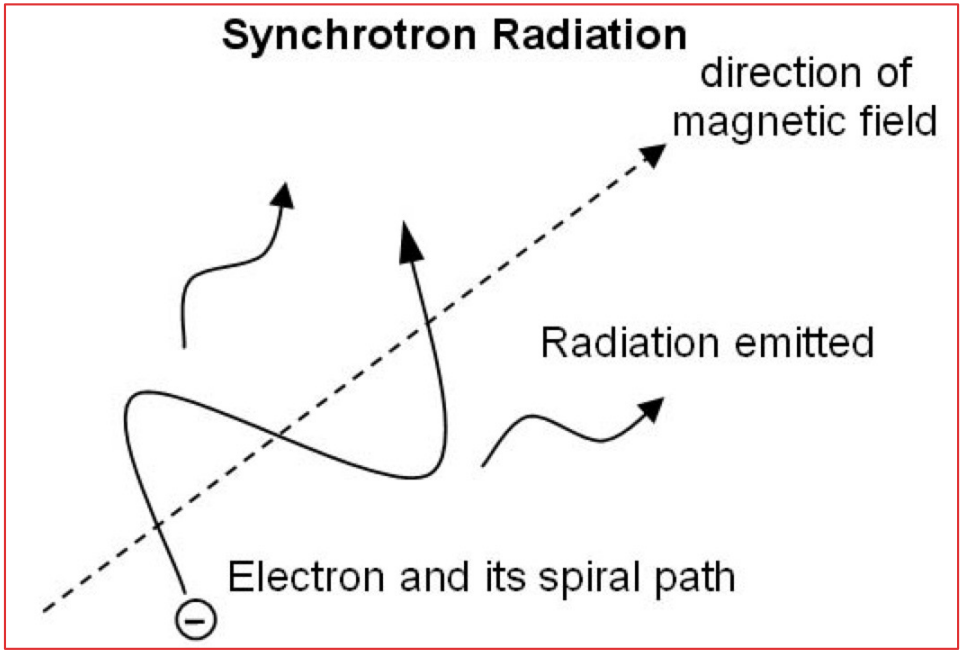

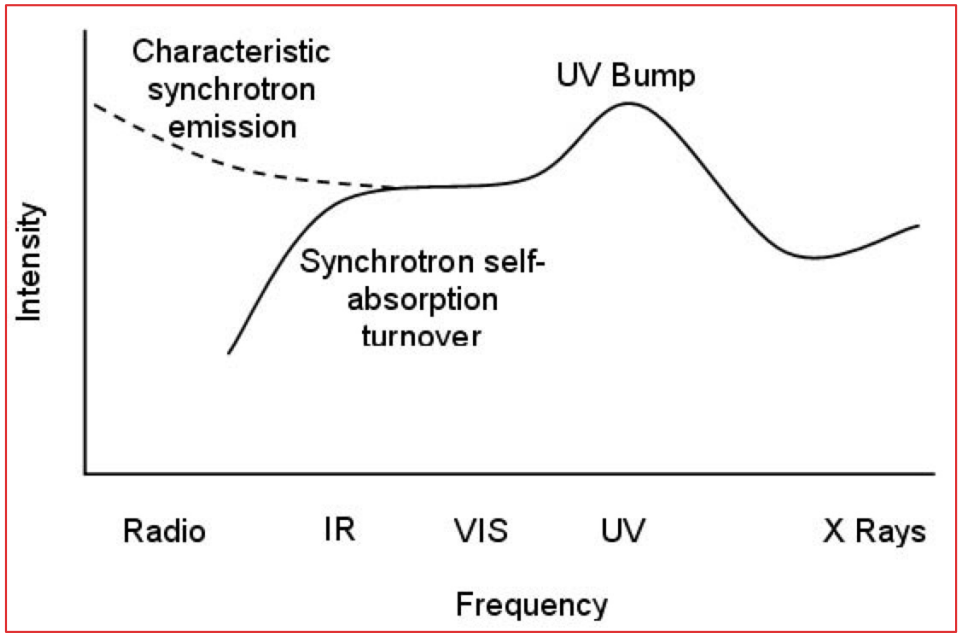

Bremsstrahlung Radiation

The bremsstrahlung or free - free emission mechanism consists in the emission of a photon by a relativistic electron, $E_e=\gamma m_e c^2$, when deflected by the electrostatic interaction with another charged particle: the electrons path is deviated and it emits a photon with typical energy $E_\gamma \sim E_e/2$.
Below E_e=1 GeV bremsstrahlung gamma-rays are generated by the same electrons producing galactic synchrotron radio emission.
The bremsstrahlung radiation arises when free electrons that have a thermal distribution of energies (a spread of energies around a mean value relating to their temperature) interact with the Coulomb field of a nucleus. This produces a characteristic spectrum that can be readily identified.
The interaction cross section is proportional to:

$$\sigma_{Brems} \propto Z^2 \alpha_{EM}^3$$

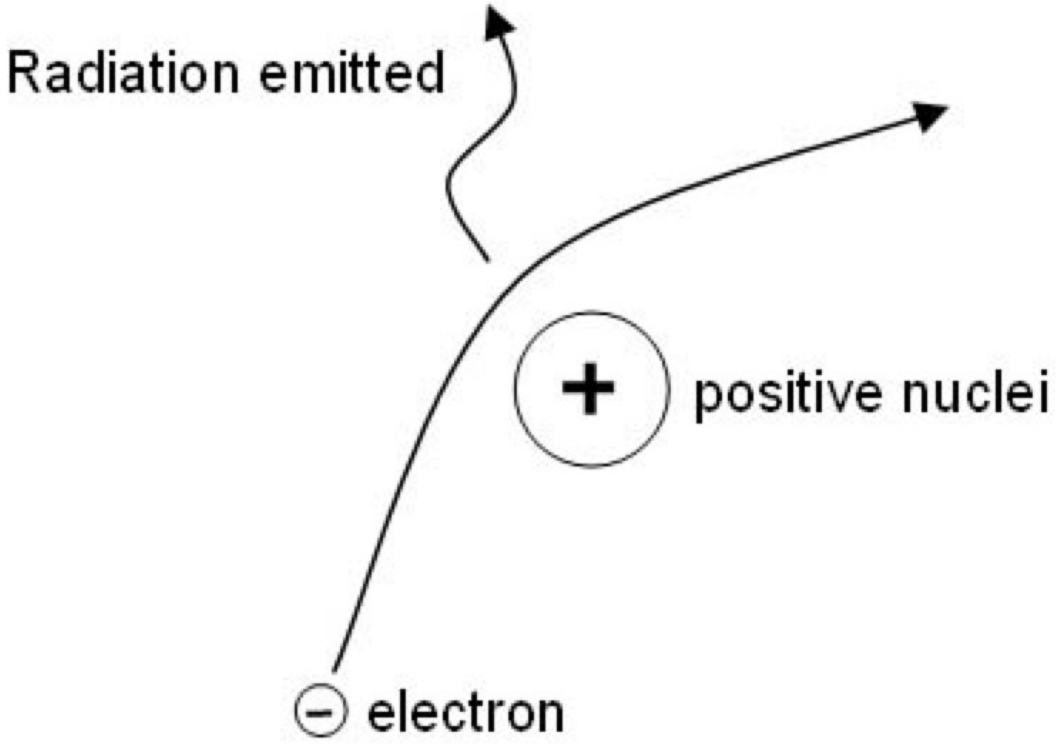

$$-\left(\frac{dE}{dt}\right)_{Brems} = 4nZ^2 R_e^2 \alpha g E \propto nE$$

where R_e is the classical electron radius, α is the fine structure constant and g is a factor (Gaunt) that changes its value according to nuclear screening fraction

Searching for astrophysical photons

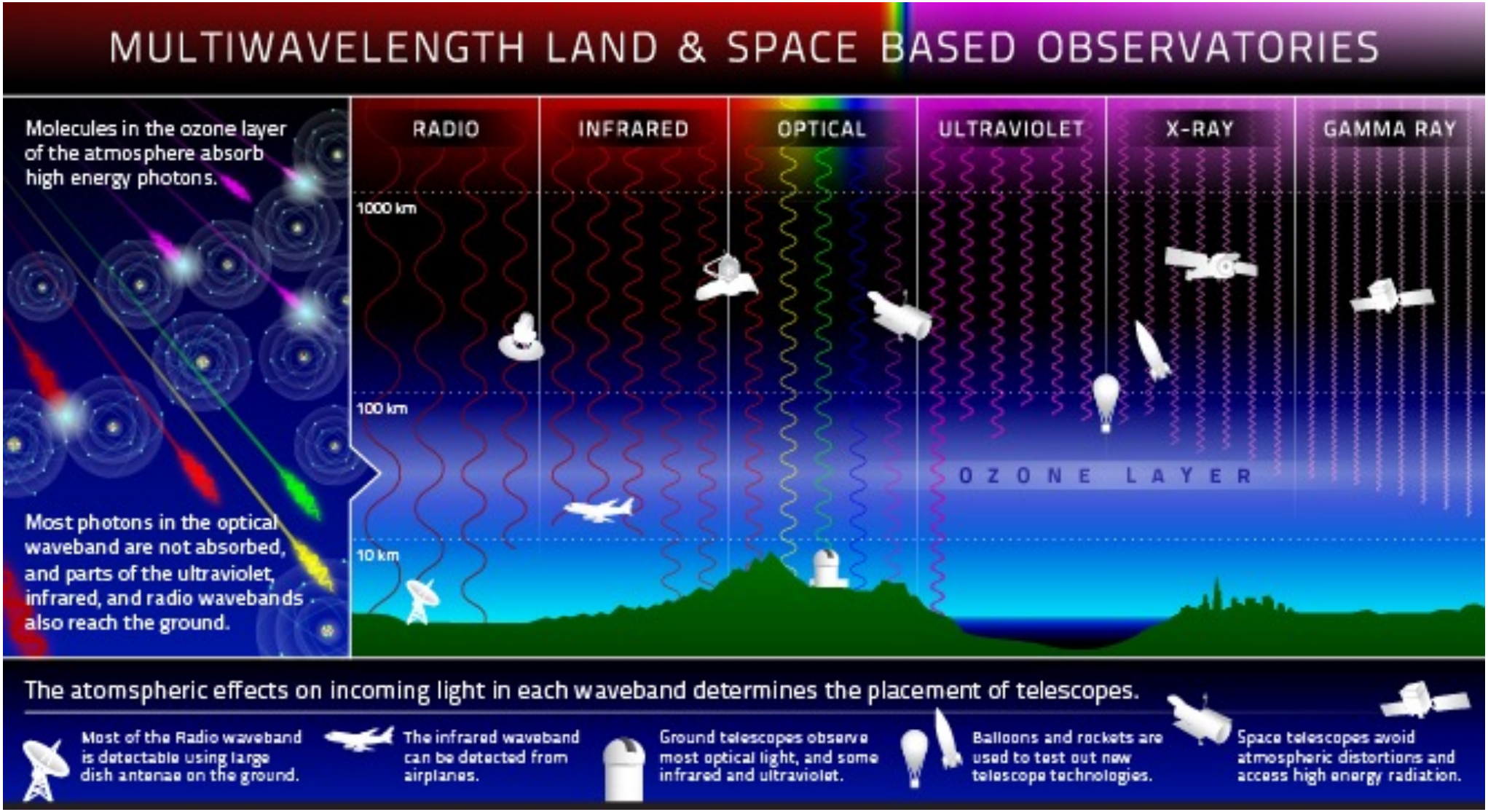

Which processes characterize the High Energy sources

leptonic process

Inverse Compton scattering

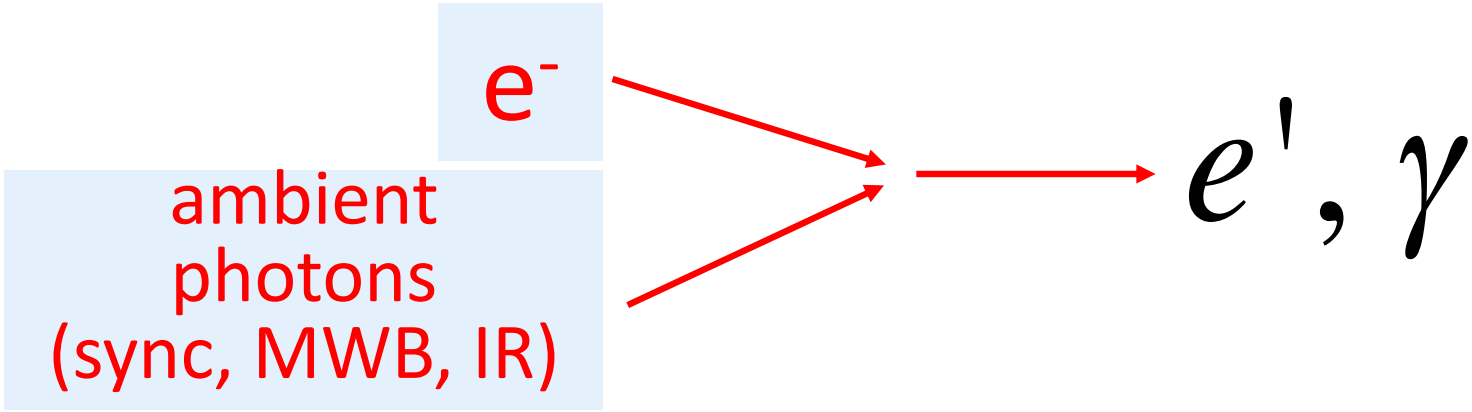

We have to consider also hadronic processes like:

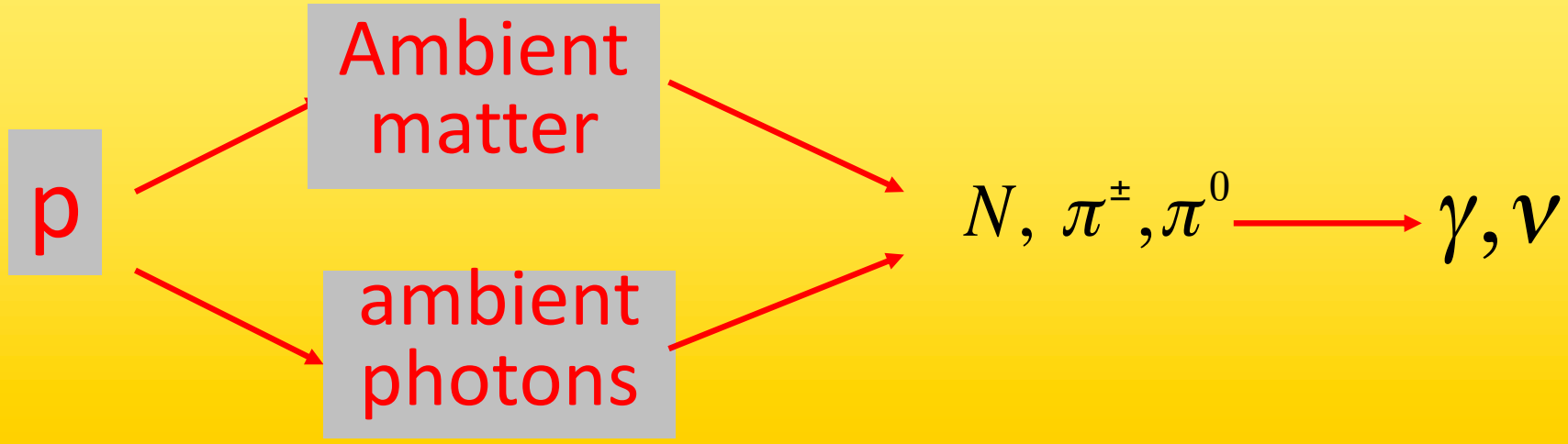

Synchrotron Self-Compton gamma production model

The most successful theories to describe the observed gamma spectra predicts an expanding ultra-relativistic shell that moves into the external surrounding medium. The collision of the expanding shell with another shell (internal shocks) or the interstellar medium (external shocks) gives rise to radiation emission through the Synchrotron and Synchrotron Self-Comtpon processes.

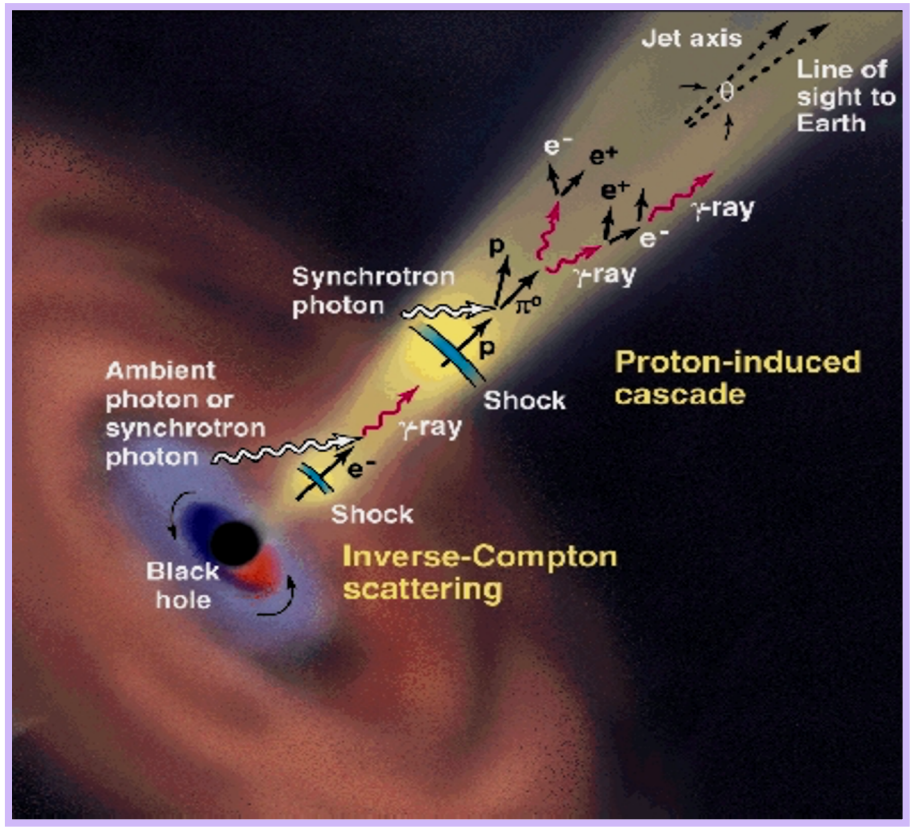

Compton and Inverse Compton scattering

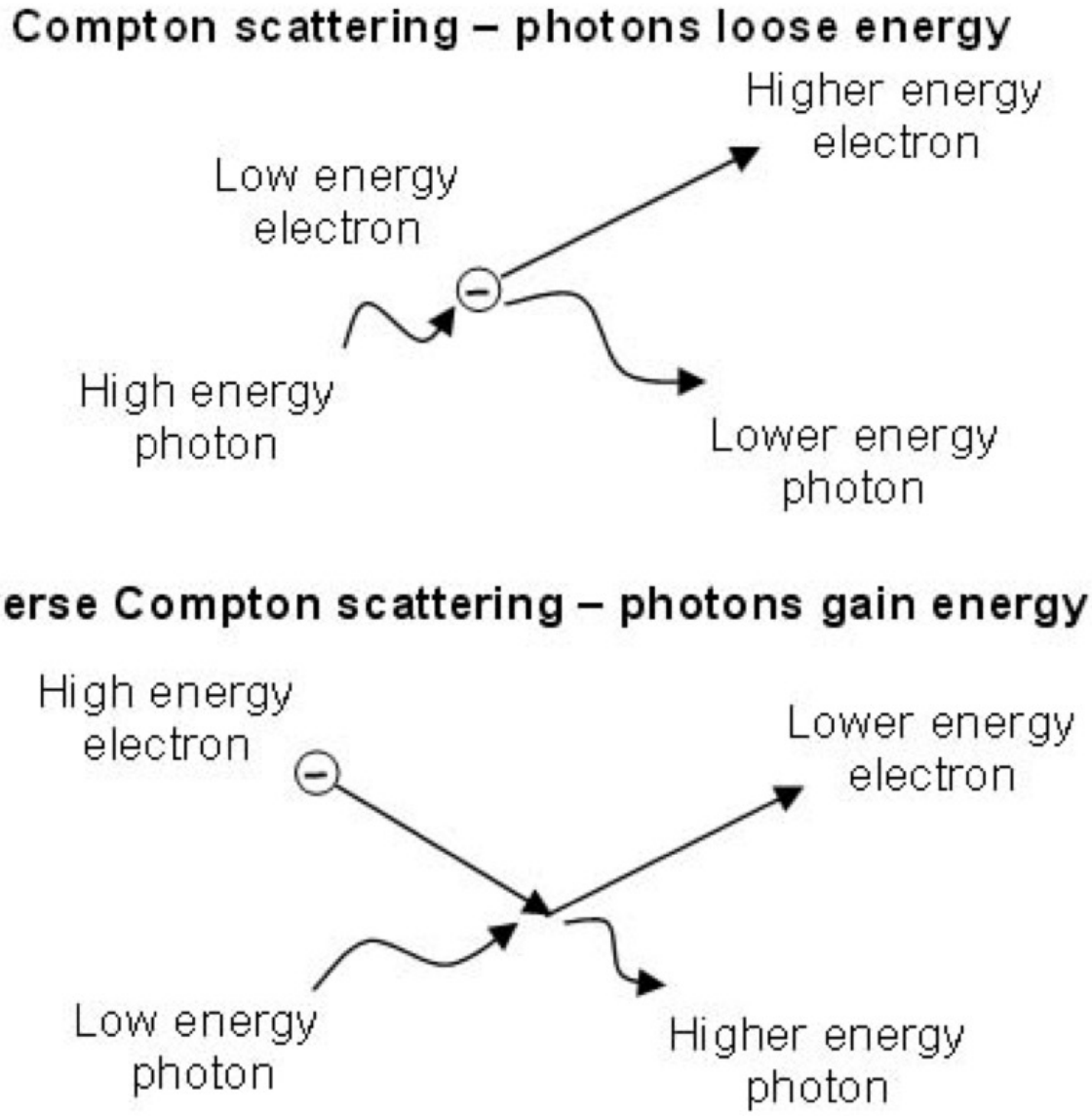

A detector for the study of primary cosmic rays with E≤ 100GeV

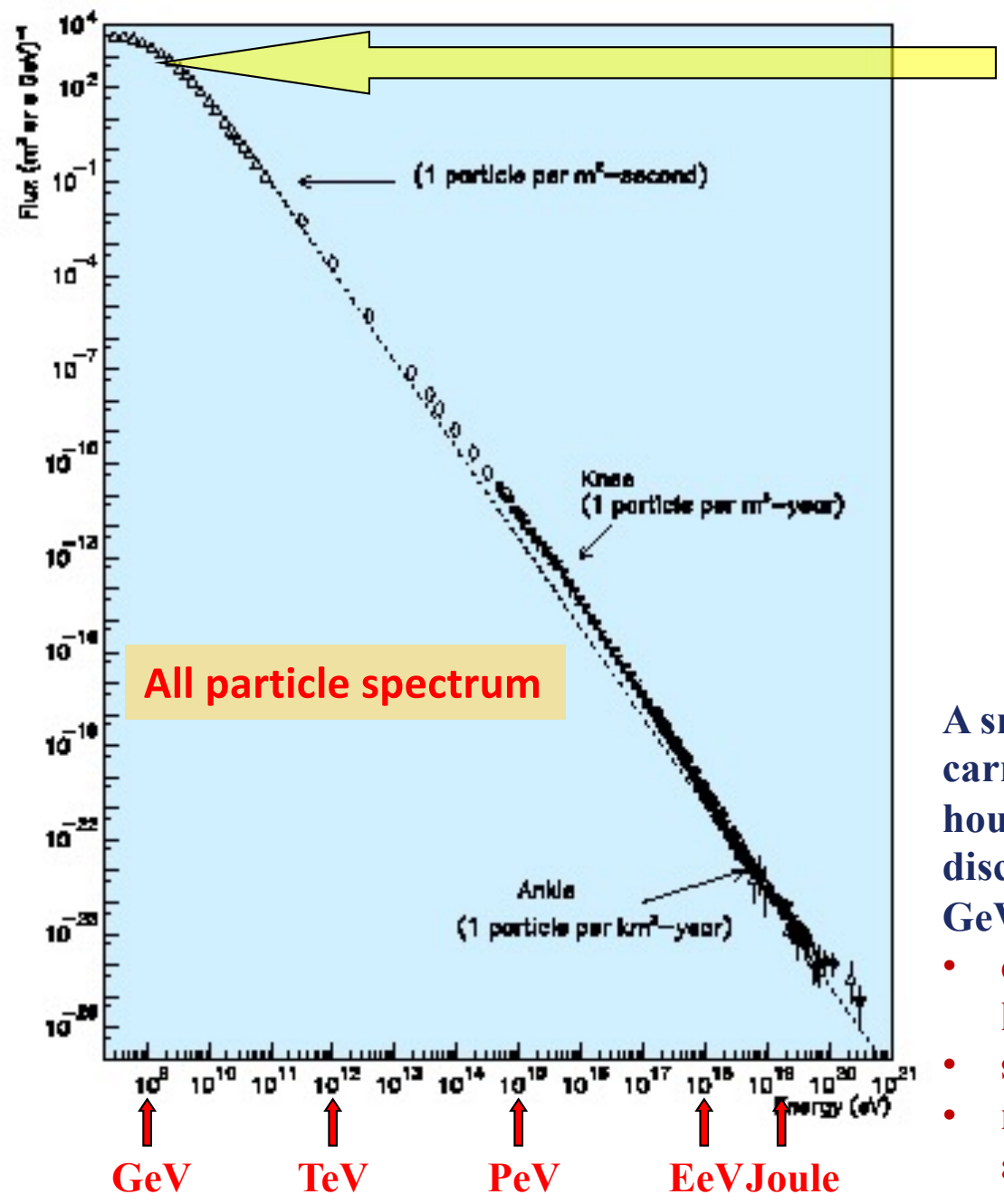

~ 10 particelle/s

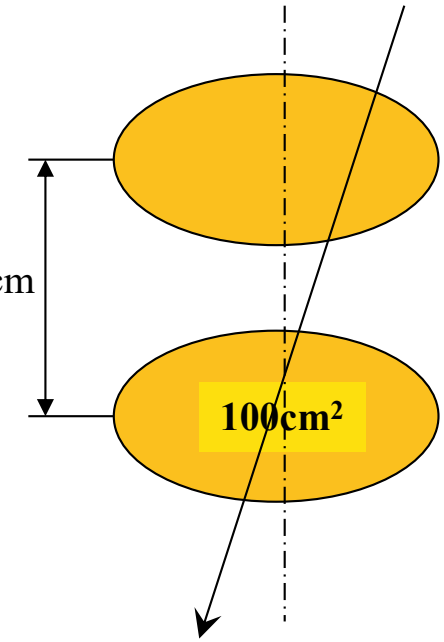

scintillators,
wire chambers,
tracking devises ,
magnetic field,
Cherenkov, ...

A small apparatus (r ~ 6cm, aperture ~ 22 cm²sr) carried by balloons (a few tens/hundred flight hours -> more than 10^5 events) can collect a discrete statistic in the energy region up to ~ 10 GeV: 100 x 22·10^{-4} x 100 x 3600 = 7.9·10^5

- **composition of cosmic rays (photons, protons, heavy nuclei, ...)**
- **spectrum**
- **matter/antimatter (identification of positrons, antiprotons, anti-helium, ...)**

Cosmic Rays detectors

All cosmic ray detectors are constructed according to a common pattern; they are generally composed of the following sub-detectors:

1. a detector consisting of two "distant" planes which measures the position and time of the passage of the particle ➔ the particle velocity measurement;
2. a detector in a magnetic field that tracks the curved trajectory of the particle ➔ a measure of rigidity;
3. a high Z detector in which particles deposit their energy ➔ a measure of energy.

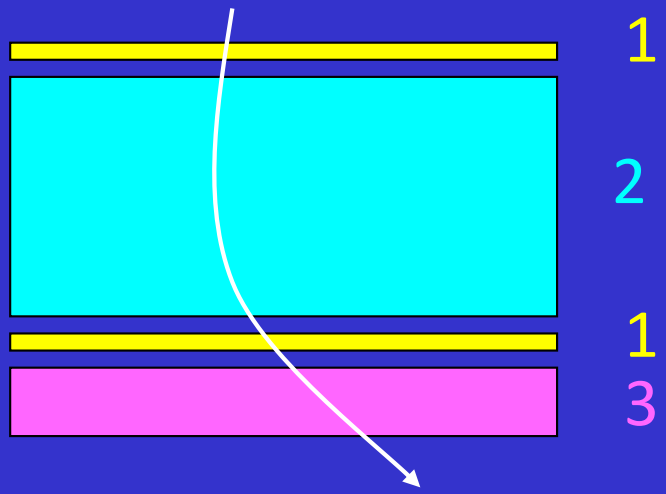

AMS, a complete detector for primary C.R.

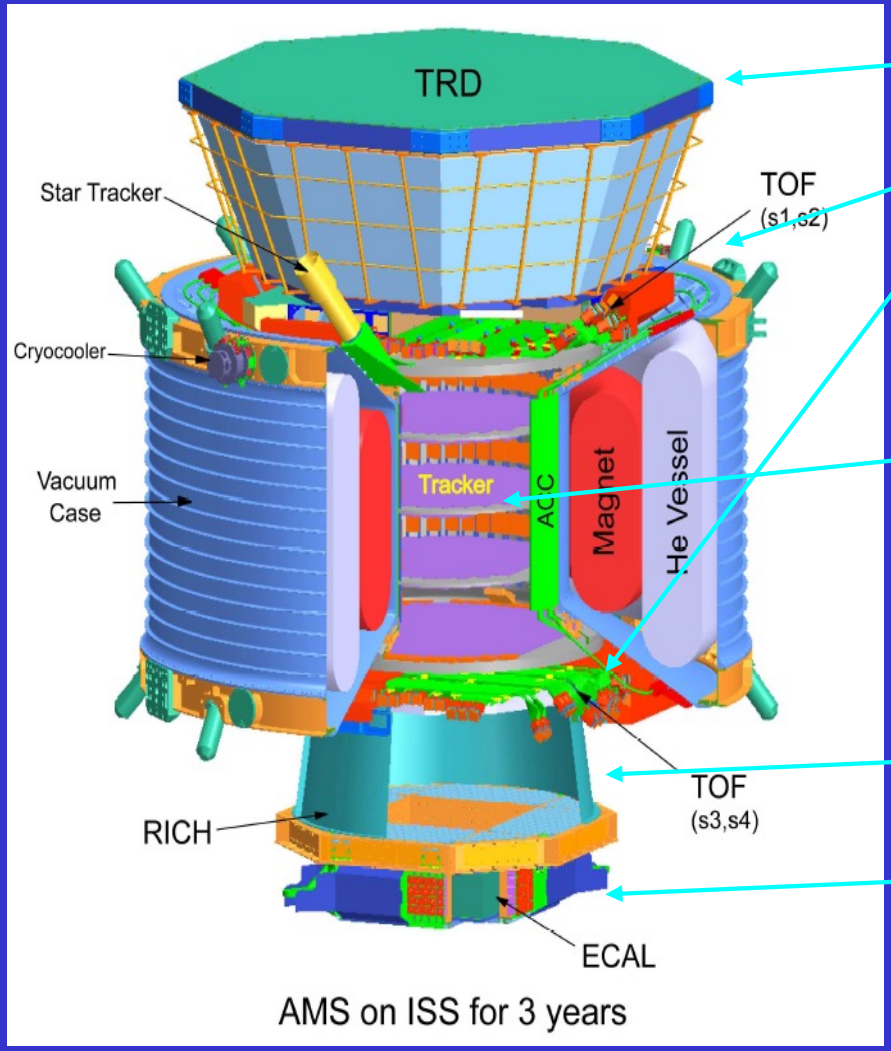

transition radiation detector

Time of flight measurement (scintillators)

tracking devise in a magnetic field

Cherenkov light detector

Electromagnetic calorimeter

Cosmic Rays detectors: momentum measurement - 1

Consider a region in which there is an electric field $\vec{E}$ and a magnetic induction field $\vec{B}$. A charge particle q = Ze in motion with speed $\vec{v}$ in that region undergoes a force equal to: $\vec{F} = q\left(\vec{E} + \vec{v} \times \vec{B}\right)$

Let θ be the angle between $\vec{v}$ and $\vec{B}$. Suppose that the particle has mass m ($m = \gamma m_0$). Now suppose that only the magnetic induction field is present:

$$\vec{F} = q\vec{v} \times \vec{B} = ZevB\sin\theta(-\hat{r}_L) = -m\frac{v^2}{r_L}\hat{r}_L = -\gamma m_0 \frac{v^2}{r_L}\hat{r}_L$$

where r_L indicates the radius of Larmor. Projecting on r_L we have:

$$ZevB\sin\theta = \gamma m_0 \frac{v^2}{r_L} \quad \rightarrow \quad r_L = \frac{\gamma m_0 v}{ZeB\sin\theta}$$

It is defined "Rigidity of a particle in a magnetic field"

$$R = \frac{\gamma m_0 v}{q}c = \frac{\gamma m_0 vc}{Ze}$$

This quantity has the dimensions of an energy divided by the charge and is measured in GV. Based on this definition we can write:

$$r_L = \frac{R}{Bc\sin\theta}$$

Cosmic Rays detectors: momentum measurement - 2

Momentum measurement

If ϑ is the angle formed by the magnetic field **B** and the particle velocity, the radius of curvature of the trajectory traveled by the particle is

$$r = R / (Bc \sin\vartheta) = (\gamma m_o v) / (Ze\, B \sin\vartheta)$$

What is usually measured is the sagitta S of the curved line which represents the trajectory of the particle (ℓ it is the length of the segment AD).

In the S << r approximation we can write:

$$\overline{AB} = r \qquad \overline{BC} = r - S = \sqrt{\left(\overline{AB}\right)^2 - \left(\frac{\ell}{2}\right)^2} \qquad S = r - \sqrt{r^2 - \left(\frac{\ell}{2}\right)^2}$$

$$S = r\left(1 - \sqrt{1 - (\ell / 2r)^2}\right) \cong \frac{\ell^2}{8r}$$

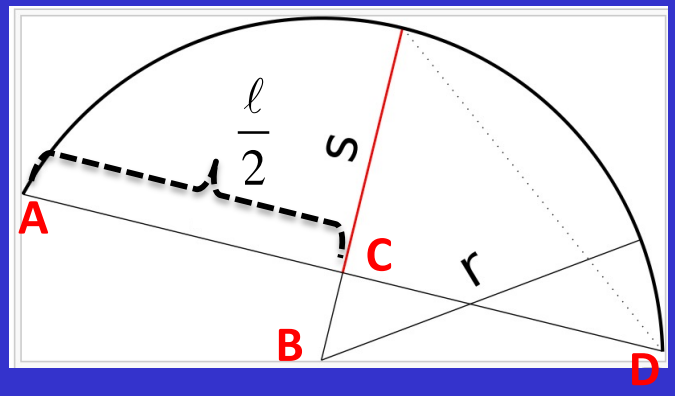

Cosmic Rays detectors: momentum measurement - 3

since it holds the relation pc = 0.3 Br, where p is the relativistic pulse expressed in GeV/c, B is the magnetic field intensity expressed in Tesla, and r is the radius of curvature in meters, we find

$$S \cong \frac{\ell^2}{8r} \Rightarrow S \propto \frac{B\ell^2}{pc}$$

$$R = r_L Bc\sin\theta \cong \frac{\ell^2}{8S} Bc\sin\theta \Rightarrow \frac{p}{ze} \cong \frac{B\ell^2 \sin\theta}{8S}$$

so we see that, with the same spatial resolution in the measurement of the sagitta, the higher the power of analysis $B\ell^2$, the greater the maximum impulse that can be measured.

Tracking detectors - 1

- Purpose: measure momentum and charge of charged particles
- To minimize multiple scattering, we want tracking detectors to contain as little material as possible
- Two main technologies:
  - gas/wire drift chambers (like CDF's COT) *
  - solid-state detectors (silicon)
- Silicon is now the dominant sensor material in use for tracking detectors at the LHC (especially CMS)

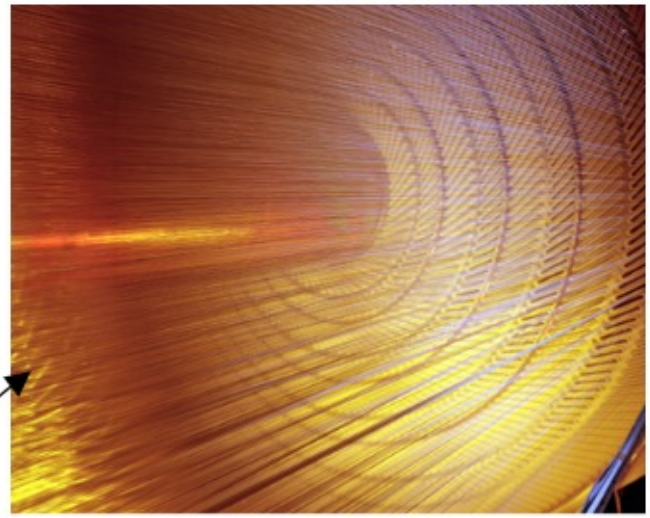

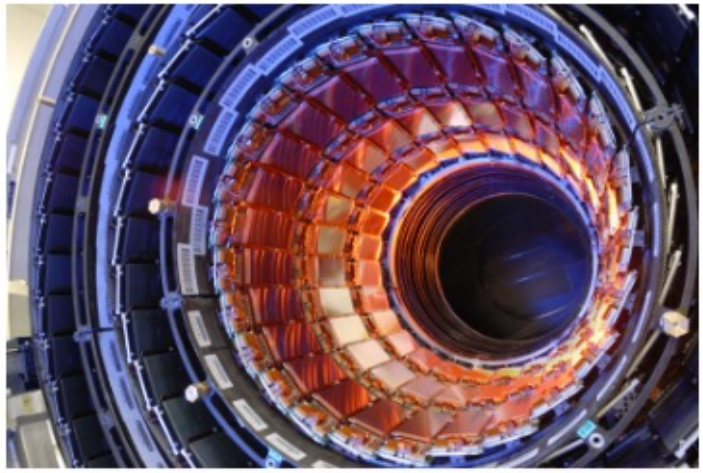

CMS

*The *CDF* Central Outer Tracker (*COT*) is a large cylindrical drift chamber, sitting inside *CDF's* 1.4T magnetic field, outside the *CDF* silicon trackers

Tracking detectors - 2

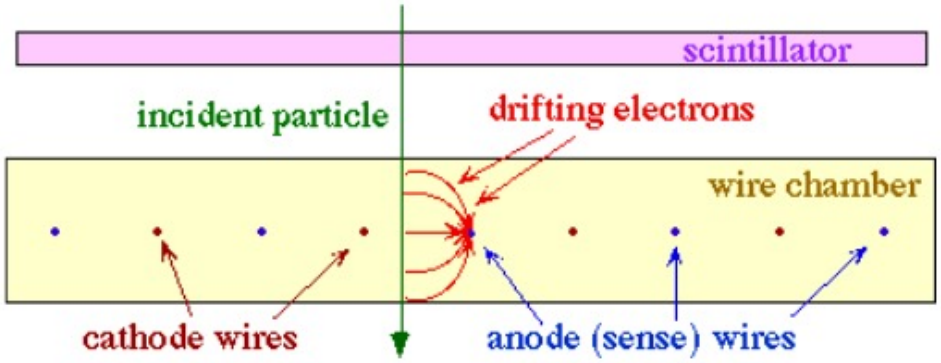

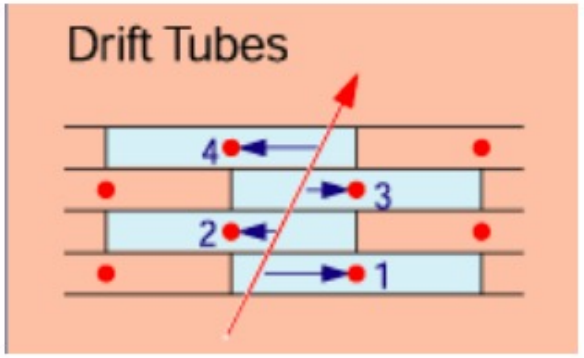

- Wires in a volume filled with a gas (such as Argon/Ethan)
- Measure where a charged particle has crossed
  - charged particle ionizes the gas.
  - electrical potentials applied to the wires so electrons drift to the sense wire
  - electronics measures the charge of the signal and when it appears.
- To reconstruct the particles track several chamber planes are needed
- Example:
  - CDF COT: 30 k wires, 180 μm *hit* resolution
- Advantage:
  - low thickness (fraction of X_0)
  - traditionally preferred technology for large volume detectors

Tracking detectors – 3 silicon detectors

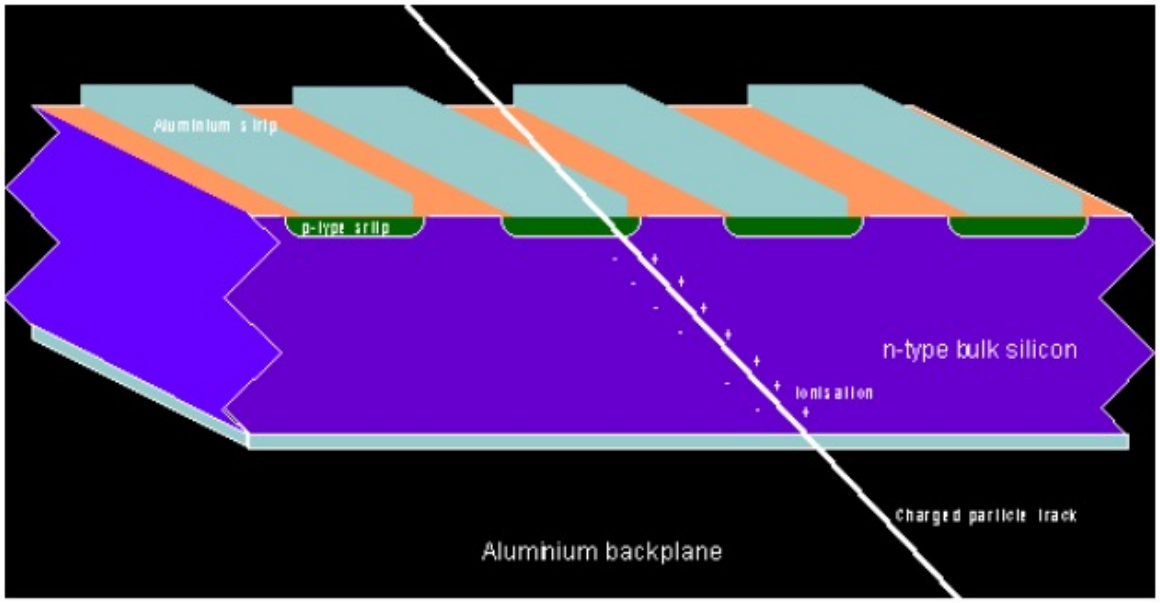

~300μm

- Semi-conductor physics:
  - doped silicon: p-n junction
  - apply very large reverse-bias voltage to p-n junction
    - "fully depleted" the silicon, leaving E field
- Resolution 1-2% @ 100 GeV
- Important for detection secondary vertices
  - b-tagging (more on this later)

Radiation Detection
Scintillation Detectors

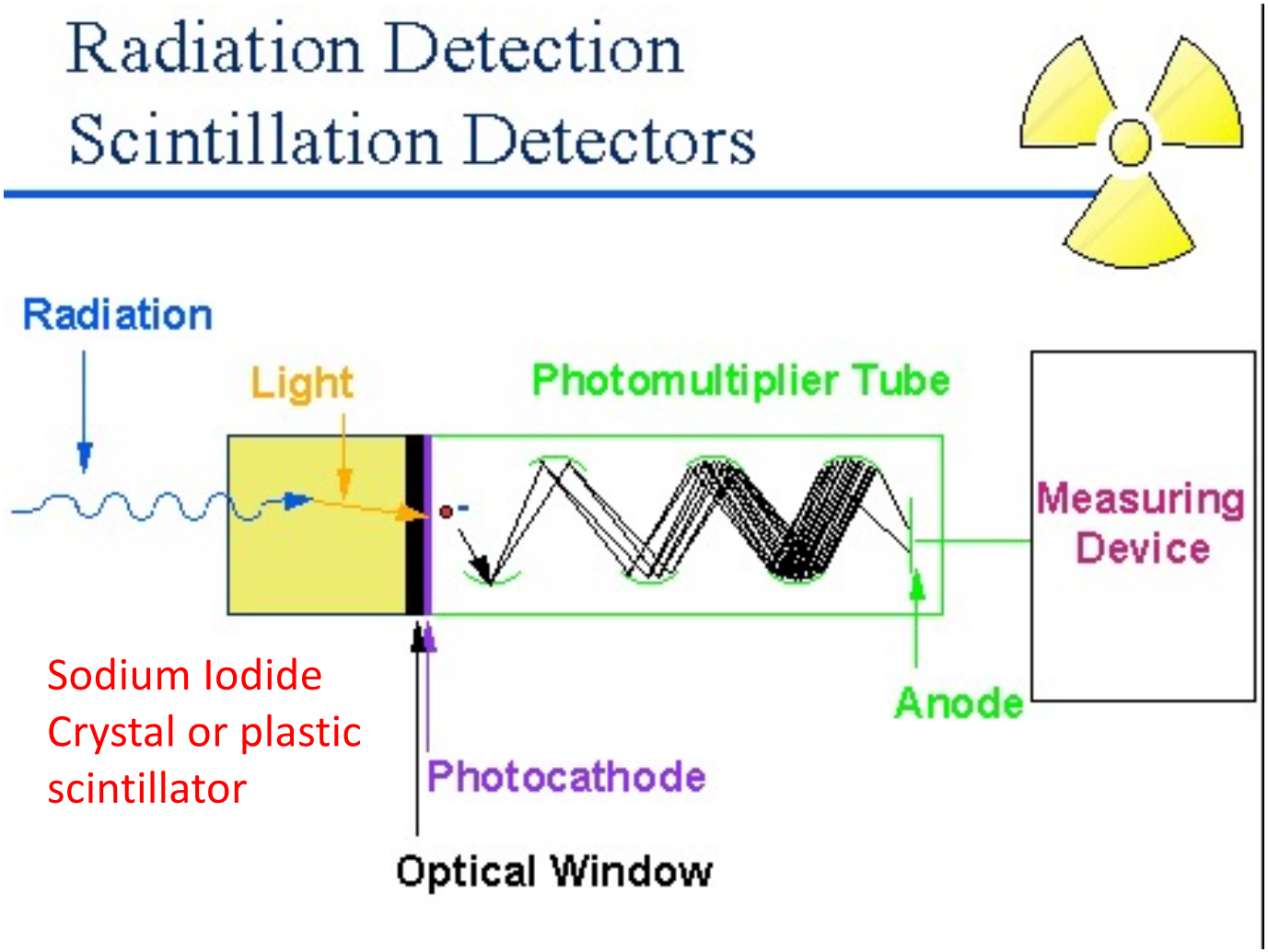

Charge measurement

The value of the nuclei electric charge is measured by the energy lost per unit of path, in fact for the very heavy particles the expression of the energy lost on average by ionization is given by the formula of Bethe-Bloch

$$-\frac{dE}{dx} = 4\pi N_e r_e^2 m_e c^2 \frac{z^2}{\beta^2}\left(\ln\frac{2m_e c^2\beta^2\gamma^2}{I} - \beta^2 - \frac{\delta(\gamma)}{2}\right)$$

- m_e and r_e are, respectively, the mass and the classical radius of the electron
- I is the ionization potential of the crossed material
- $\delta(\gamma)$ is a "density correction that, in the limit of high γ, limits the logarithmic rise of the energy losses
- β is the particle velocity in terms of the light speed

then:

$$\frac{dE}{dx} \propto z^2$$

therefore for particles at the minimum of ionization (or even more energetic) the measure of the loss of energy is essentially a measure of the absolute value of the electric charge.

Cosmic Rays mass measurement

Knowing dE / dx, function of (z, β), and the rigidity R (m_o, z, β) remains as the only unknown m_o that can be obtained with a measure of β with the time of flight system.

The particle identification system is so complete.

Calorimetric measurements of shower energies -1

E.M. Showers development (basic concepts in e.m. calorimeters)

- **e.m. showers formation e.m.**
  - particle multiplication processes

    $e \rightarrow e'\gamma$

    $\gamma \rightarrow e^+e^-$
  - energy degradation processes
  - multiple scattering
  - radiation absorption

- **conversion into visible energy of the deposited kinetic E_{dep}**
  - Ionization
  - production of electron-hole pairs
  - molecular atomic excitation

    absorption in luminescent centres

    return to the ground state with photon / phonon emission

  - Cerenkov light emission
  - energy conversion into thermal phonons

Calorimetric measurements of shower energies -2

- Purpose: measure energy of EM particles (charged or neutral)
- How?
  - Use heavy material to cause EM shower (brem/pair production)
  - Total absorption / stop particles
  - Important parameter is X_0 (usually 15-30 X_0 or a high Z material)
  - There is little material before the calorimeter (tracker)
- Two types of calorimeters:
  - Sampling
  - Homogeneous
- Relative energy uncertainty decreases with E !

CMS EM Cal (PbWO)

$$\frac{\sigma_E}{E} = \frac{a}{\sqrt{E}} \oplus b \oplus \frac{c}{E}$$

a: stochastic term (photon counting)
b: constant term
c: noise (electronics)

Pictures of EM and Hadronic showers

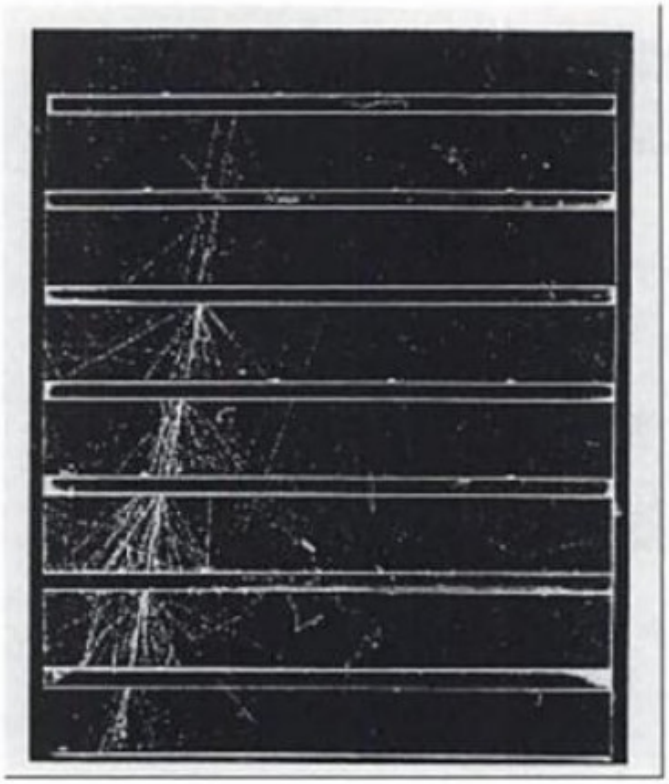

Figure 2.5 A photograph of the development of an electromagnetic shower in Pb plates. The number of particles in the shower builds up geometrically. After reaching a maximum, the shower then slowly dies off due to ionization loss ([2] – with permission).

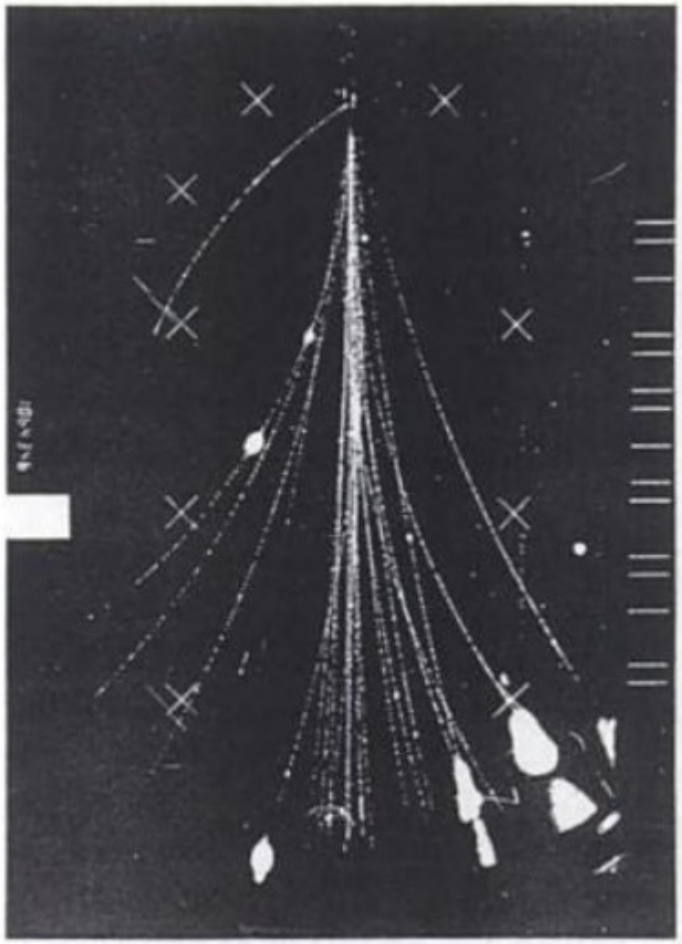

Figure 2.10 Photograph of a 200 GeV pion interaction ([5] – with permission).

Calorimetric measurements of shower energies -3

- Sampling calorimeter
  - active medium which generates signal
    - scintillator, an ionizing noble liquid, a Cherenkov radiator…
  - a passive medium which functions as an absorber
    - material of high density, such as lead, iron, copper, or depleted uranium.
    - σE/E ~ 10%

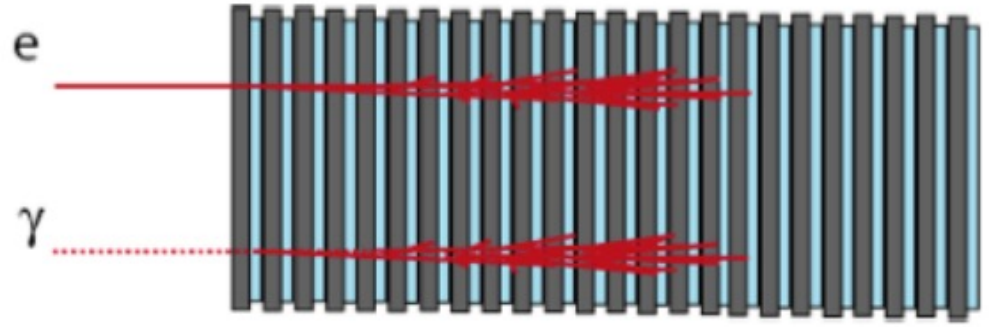

- Homogeneous calorimeter
  - the entire volume generates signal.
  - usually electromagnetic
  - inorganic heavy (high-Z) scintillating crystals
    - CsI, NaI, and PWO, ionizing noble liquids…
    - σE/E ~ 1%

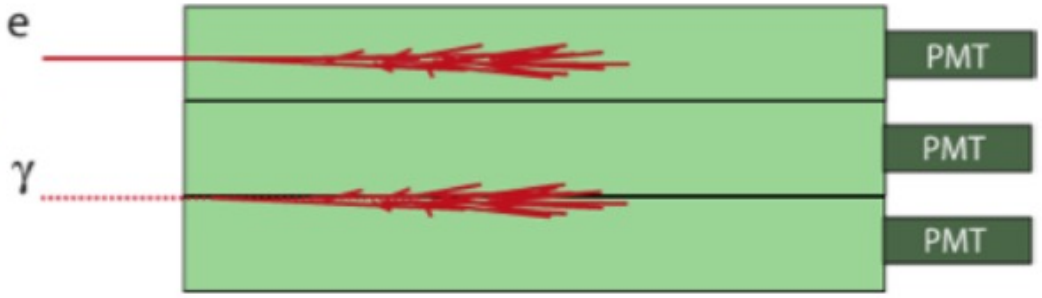

AMS - a cosmic rays detector

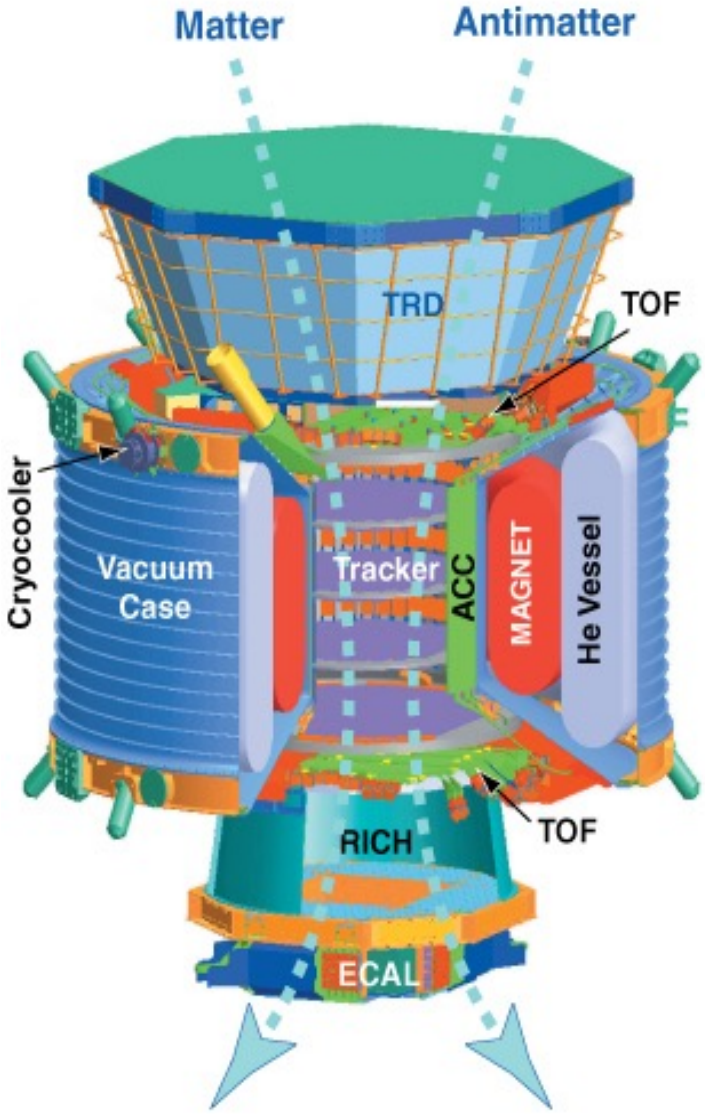

300,000 channels of electronics $\Delta t = 100$ ps, $\Delta x = 10\mu$

0.3 TeV	e^-	e^+	P	$\bar{He}$	γ
TRD					
TOF					
Tracker					
RICH					
Calorimeter					

Astronomy with R.C. and with "cosmic" photons

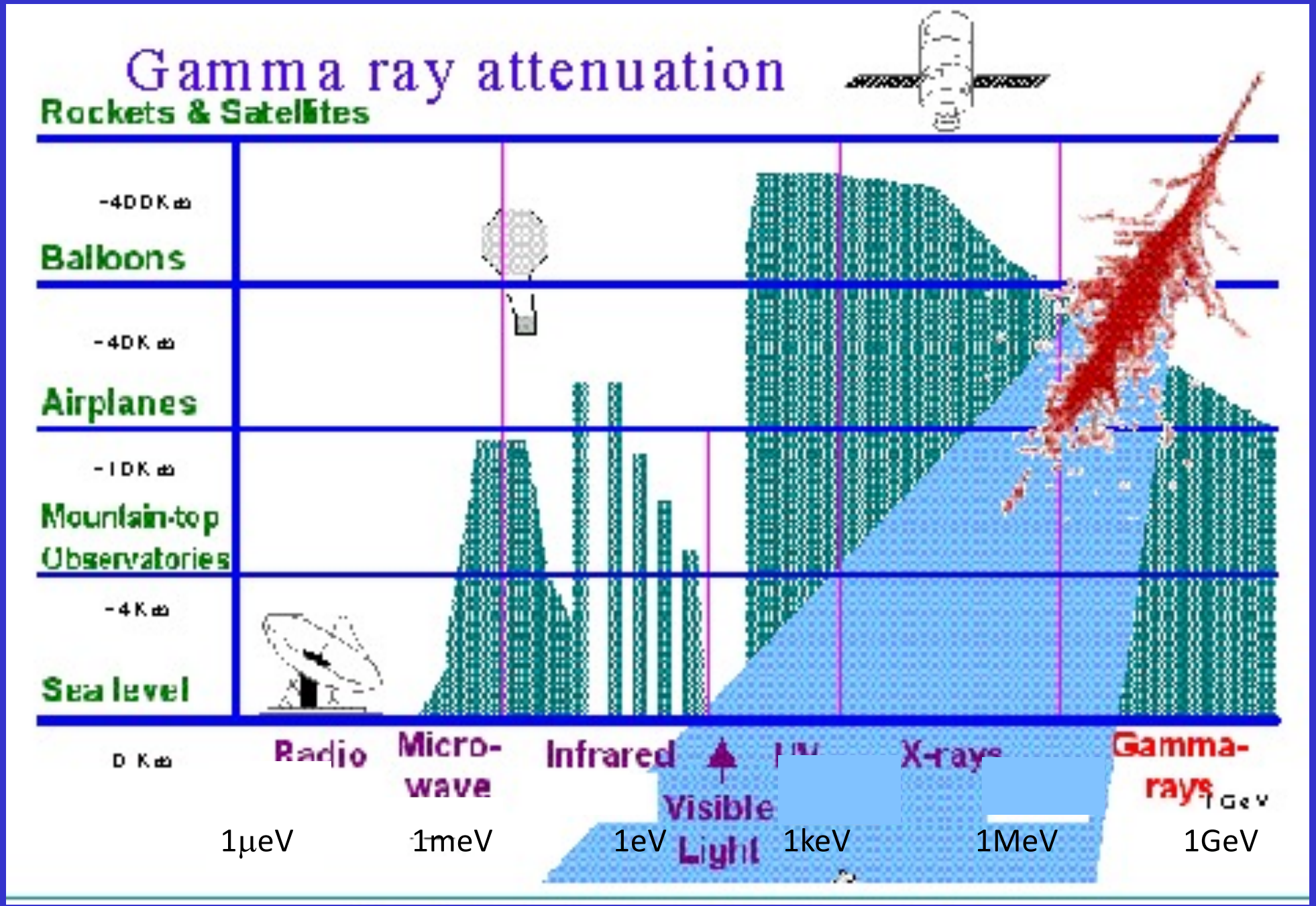

The first historical measurements of the antiproton/proton ratio

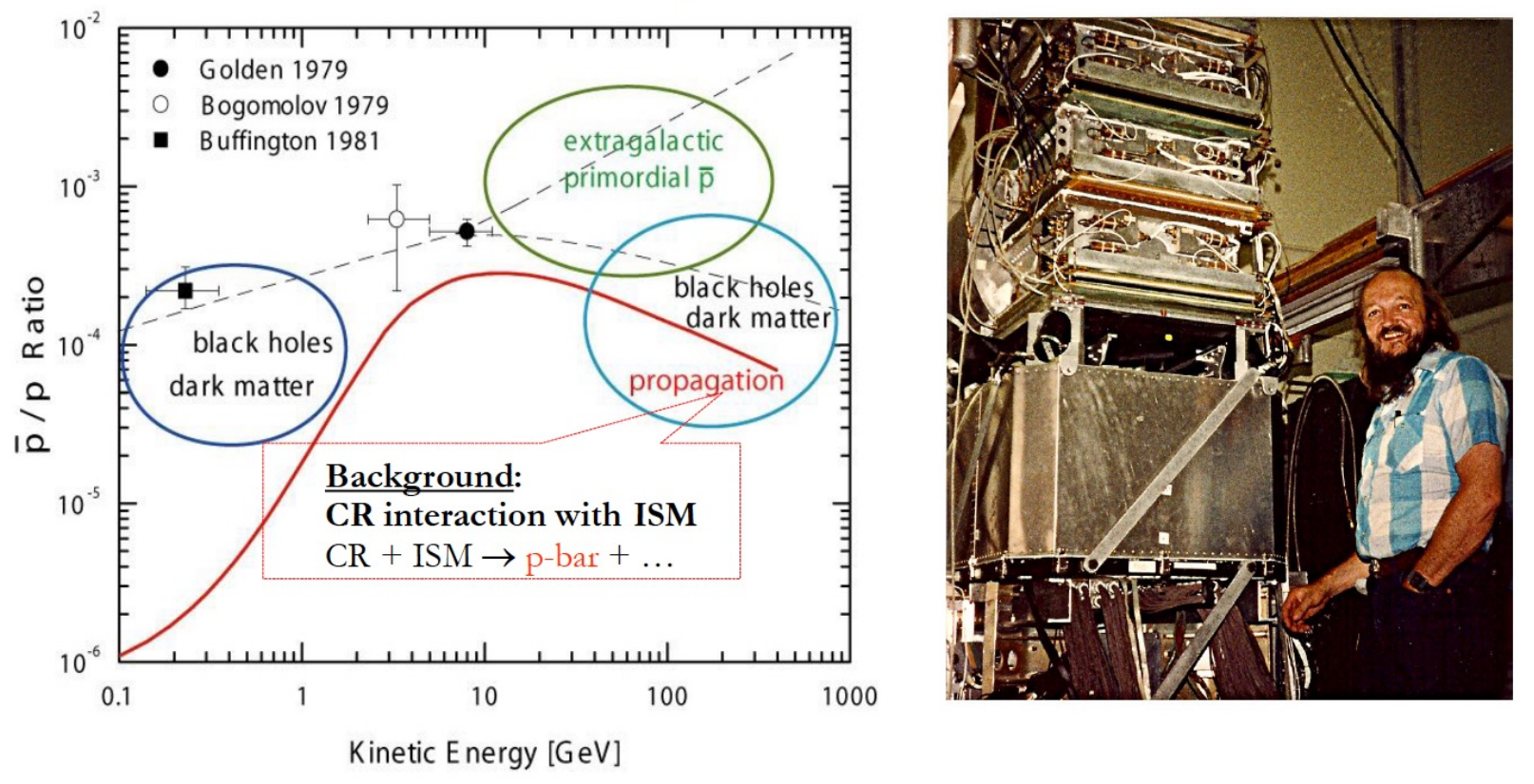

Atmospheric Balloons and C.R. physics

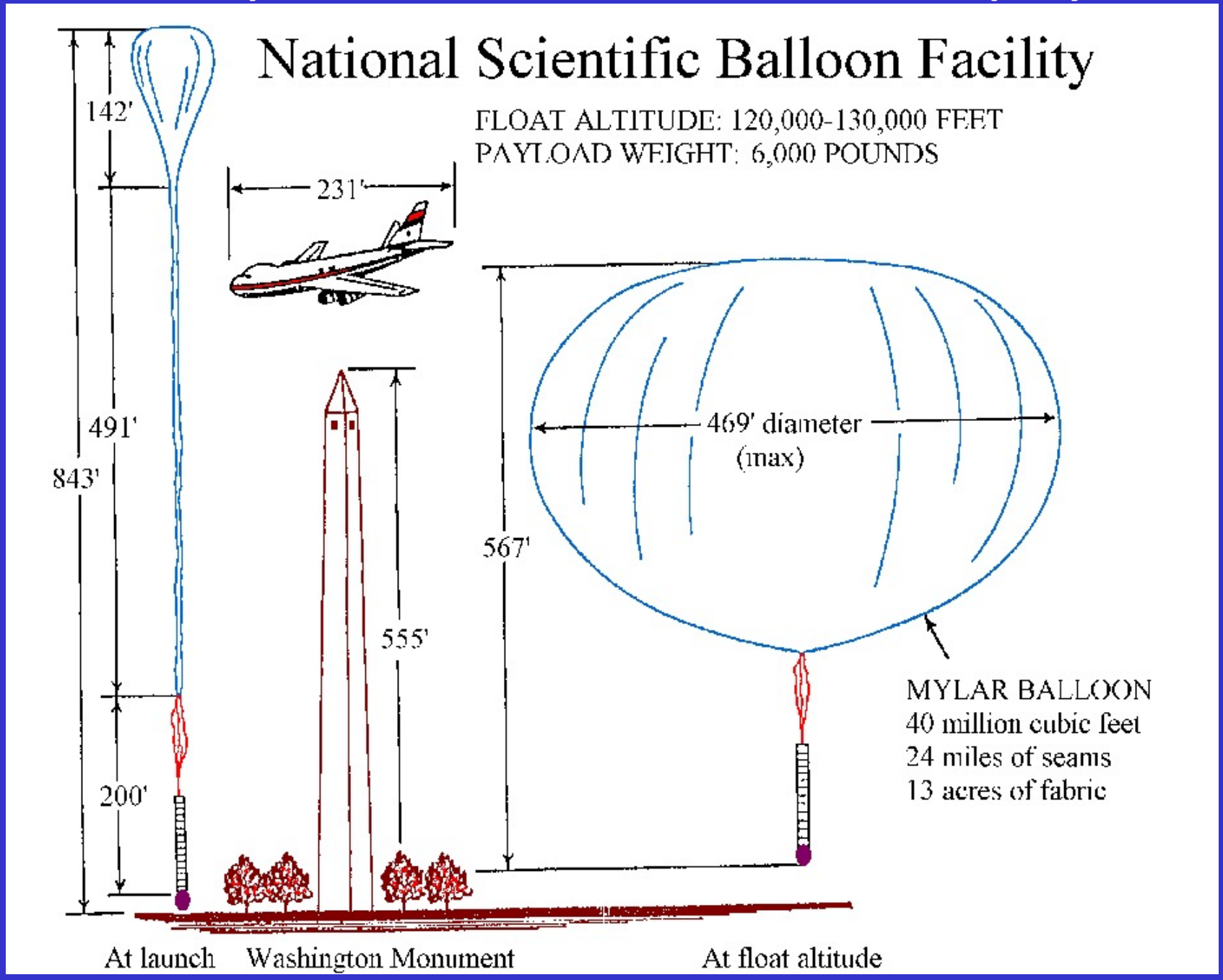

Balloon data: positron fraction before 1990

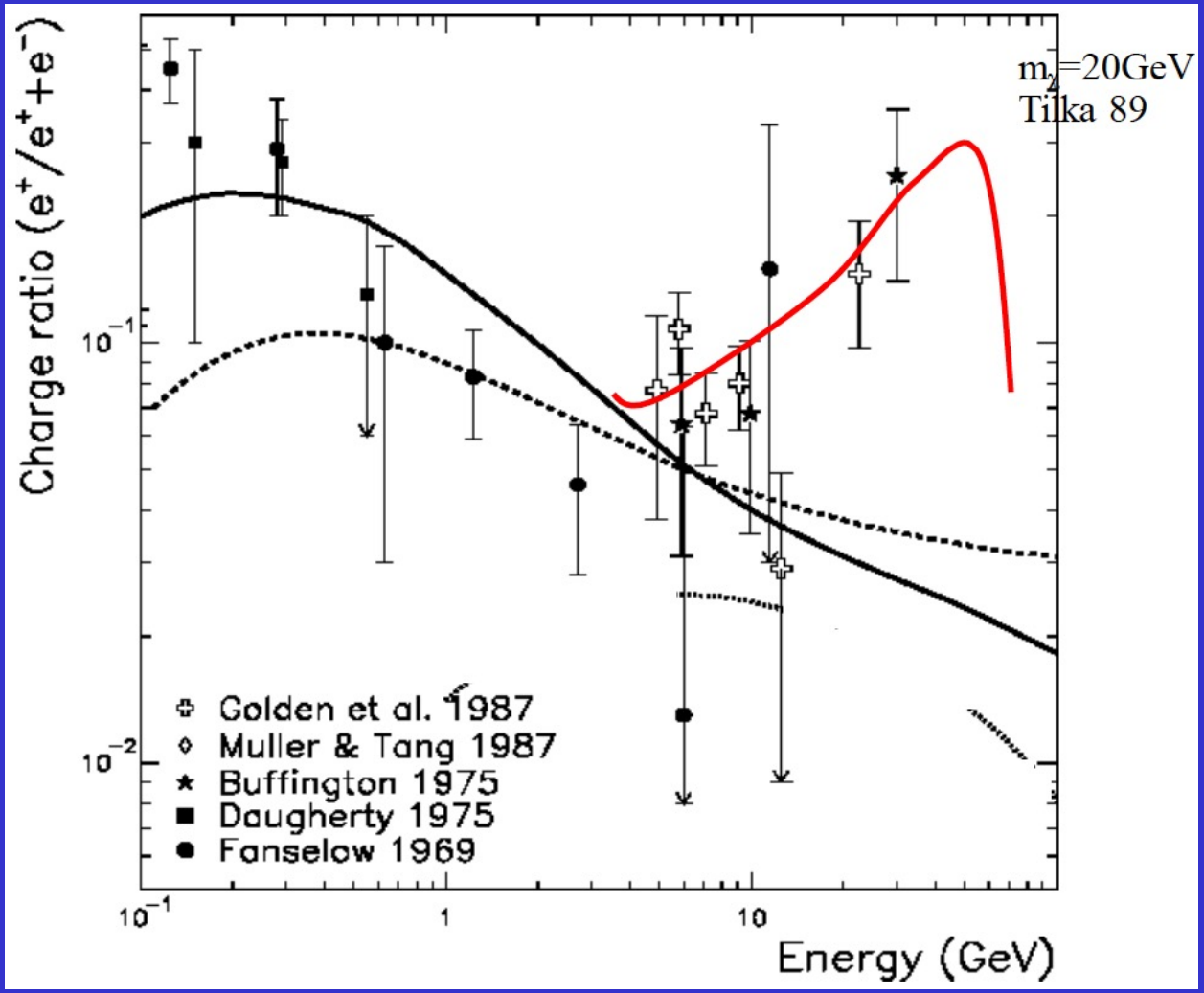

An evidence for an “excess of antimatter” ?? A first evidence of “dark matter” ?

Cosmic Rays and Antiparticles

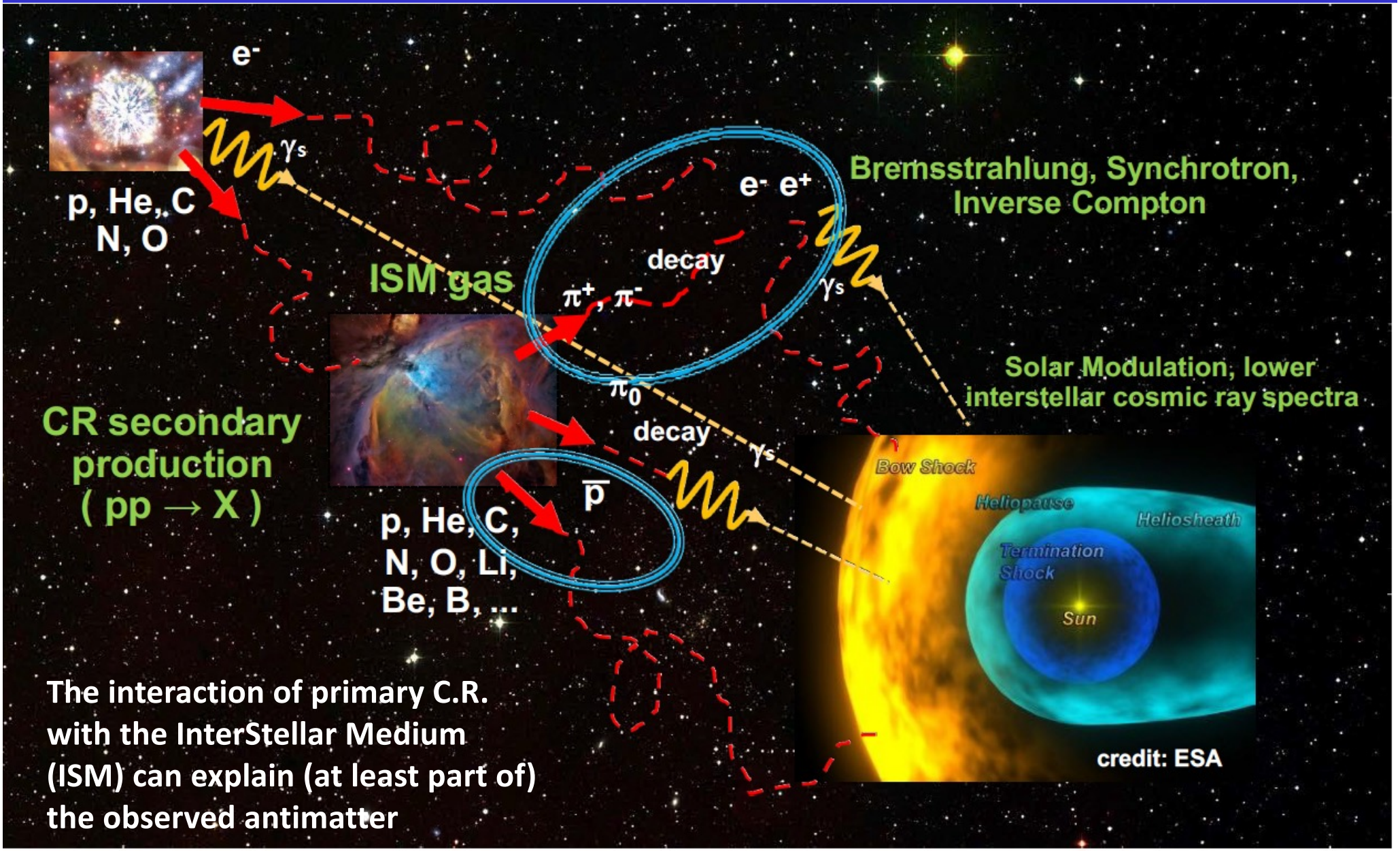

Do we expect to find an "antimatter" component in primary C.R. ?

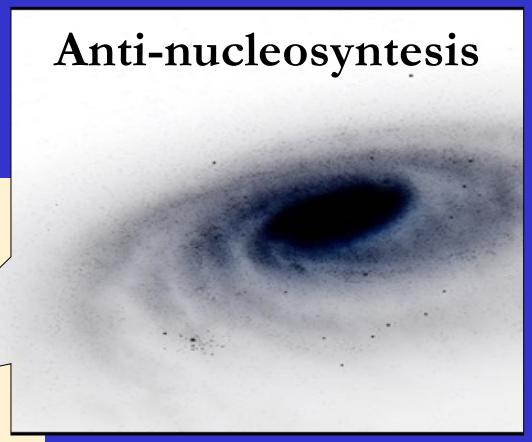

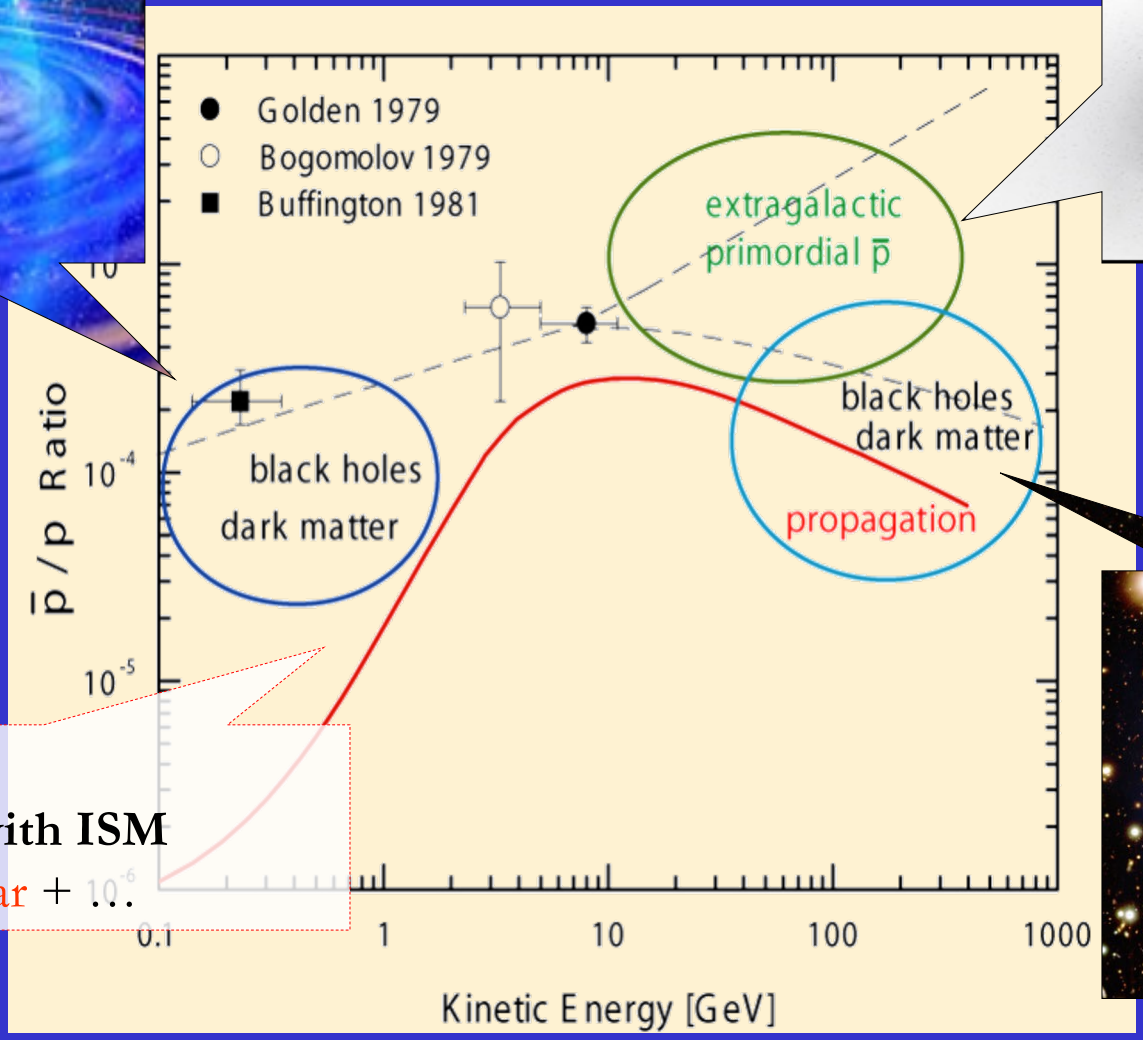

Background:
CR interaction with ISM
CR + ISM → p-bar + …

Cosmic Rays and Antiparticles

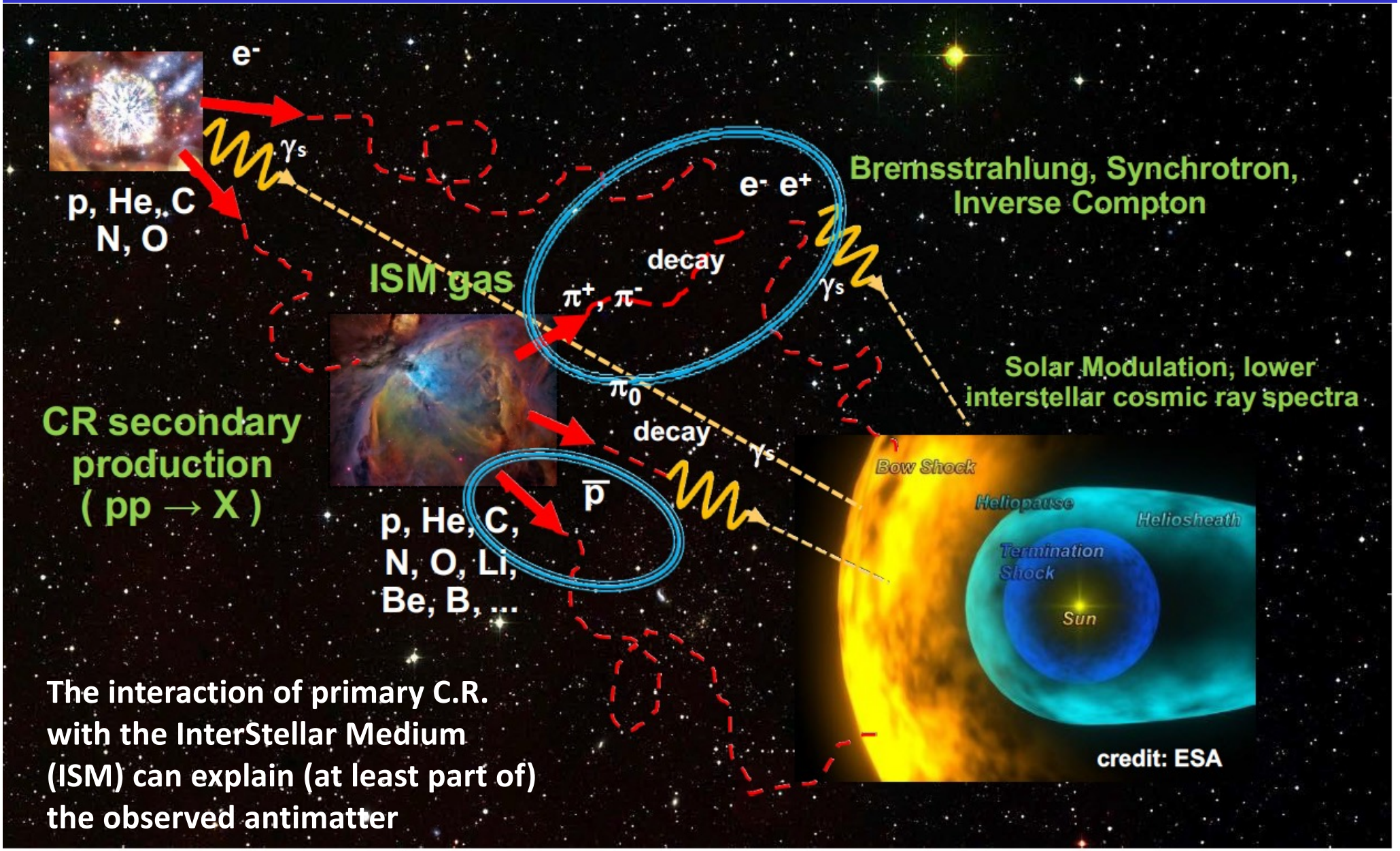

MASS - Matter Antimatter Space Experiment

Designed to measure

- antiprotons with E ~ 4-20 GeV
- positrons with E ~ 4-10 GeV.

It is the evolution of MASS1 (exp. brought in flight already in 1989), with the tracing apparatus improved thanks to a system of "drift chambers". **The identification of particles is possible thanks to the gas-Cherenkov (Freon-12) detector and to a calorimeter made of brass-streamer tubes (and Isobutane).** The experiment was carried out for 23 hours in September 1991 by Ft. Sumner, after 10 hours the magnetic field was lost.

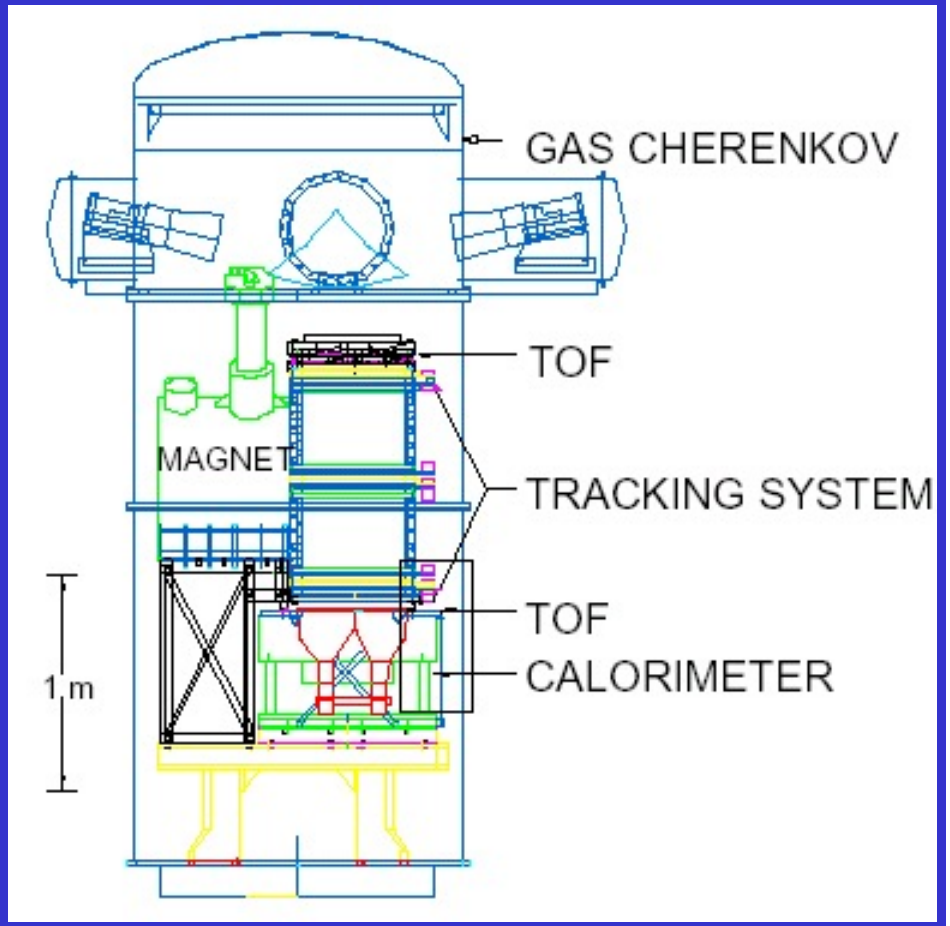

Matter Antimatter Space Spectrometer 2
MASS - 1991

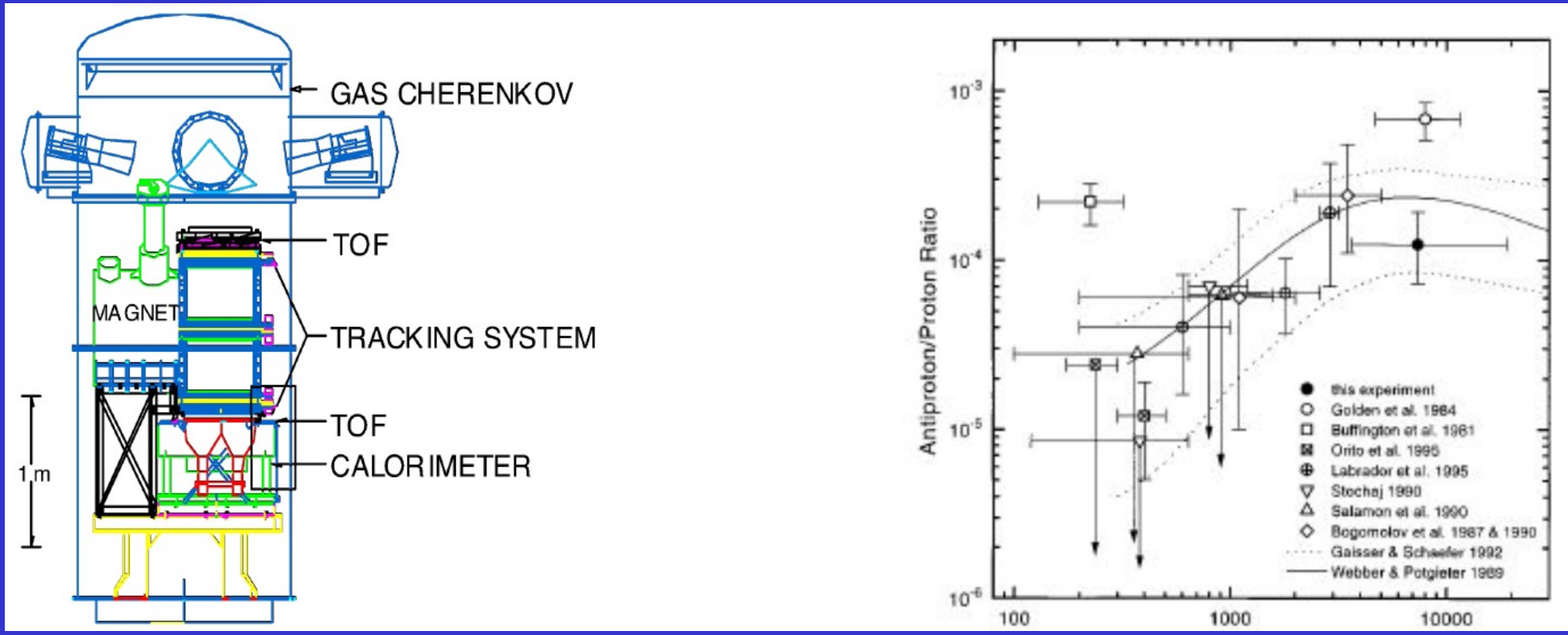

Isotope Matter Antimatter Experiment

IMAX

Made to be transported in the upper atmosphere with balloons and to measure abundance in galactic C.R. of protons, antiprotons, deuterium, helium-3 and helium-4 in the energy range ~ 0.2÷3.2 GeV/nucleon. In this region of energies there is the maximum intensity for the expected flows of the particles to be observed

IMAX measures the magnetic rigidity of charged particles that pass through the apparatus (by tracking in the drift chambers (DC) and in the multiwire proportional counters (MWPC)), the charge (via dE/dx in the scintillators (S1, S2) that provide also the time -of-flight (TOF)), and the speed (via time-of-flight (TOF) and the Cherenkov aerogel meters (C2 and C3)).

By combining these three quantities it is possible to identify the particle by mass, charge and sign of the charge.

IMAX was launched in July 1992 starting from Lynn Lake, Manitoba, Canada, has reached the quota of about 36 km (with a residual atmosphere of 5 g/cm^2) and during about 16 hours has collected more than 3 million of events (collecting a statistic 10 times greater than previous experiments).

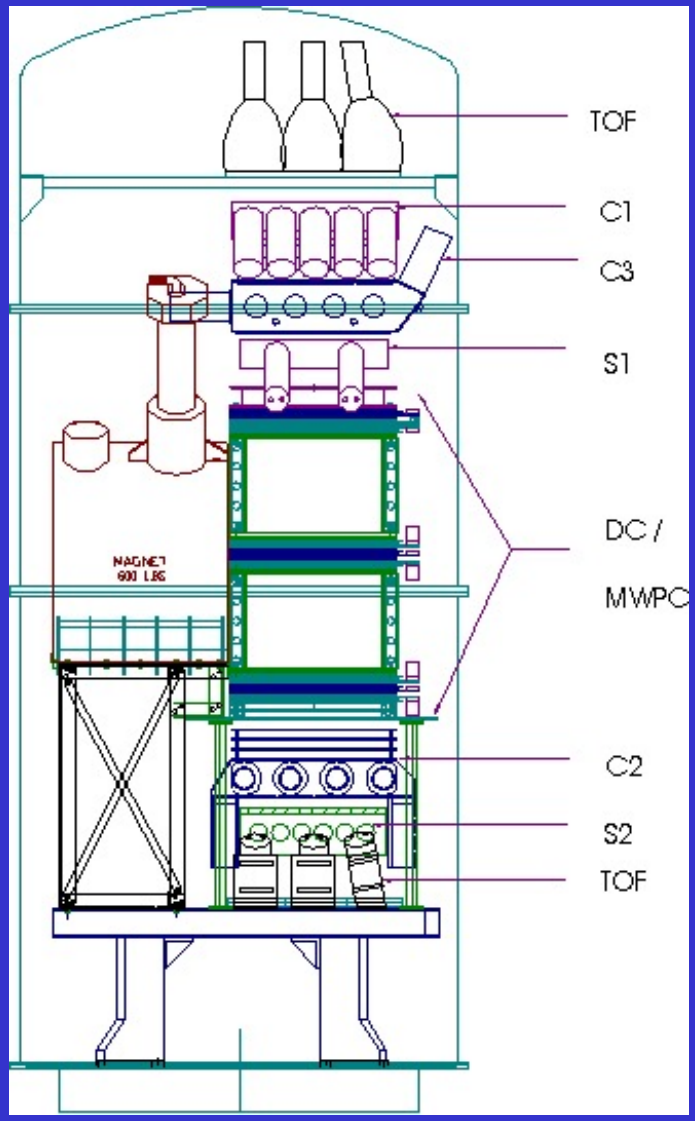

$$\text{Rigidity} = p\,c/Ze\ [GV] = [\text{energy/charge}]$$

$$\sin\theta/2 = Ze\,B\,L/(2\,p) = B\,L\,c/(2\,R)$$

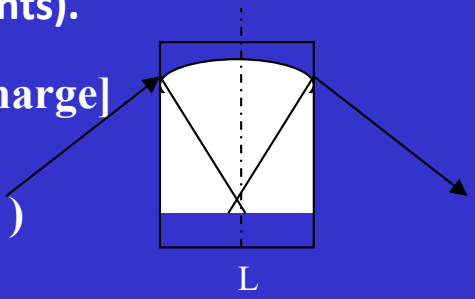

IMAX – the flight

FLIGHT

16-17 July 16-17, 1992, Lynn Lake, Manitoba, Canada. Float was reached about 7 hours after launch. The instrument took data throughout ascent, recording about 1.4×10^6 events. These data will be used to determine altitude-dependent particle spectra. At the end of the float period, the magnet was ramped down and data was taken with the magnet off in order to check the alignment of the tracking chambers. Landing was near Peace River, Alberta, Canada, with the instrument being recovered in excellent condition. All payload and detector systems appear to have performed well throughout the flight. Over 3.4×10^6 events were recorded during the float period.

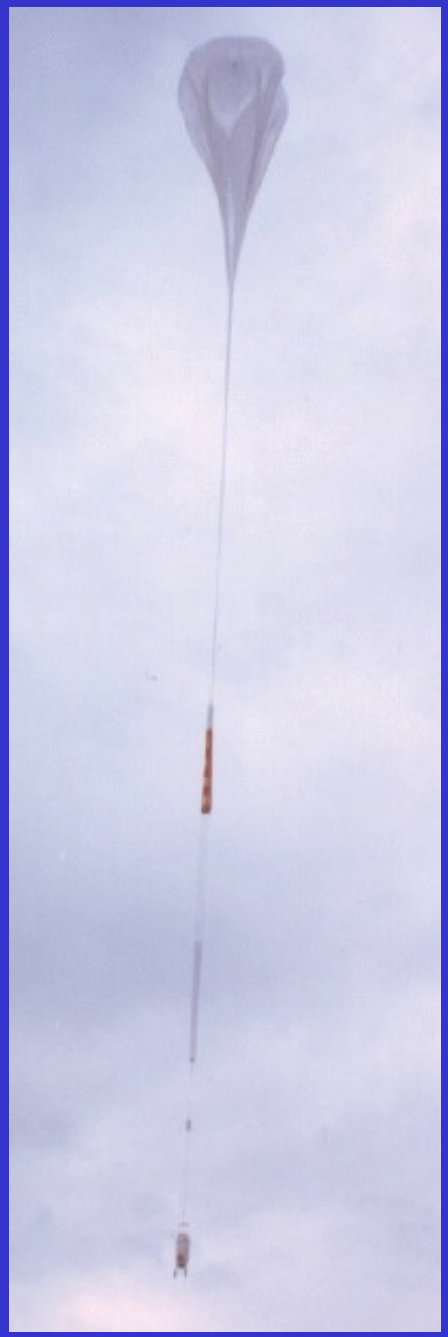

IMAX – evidence for an antiproton flux in C.R.

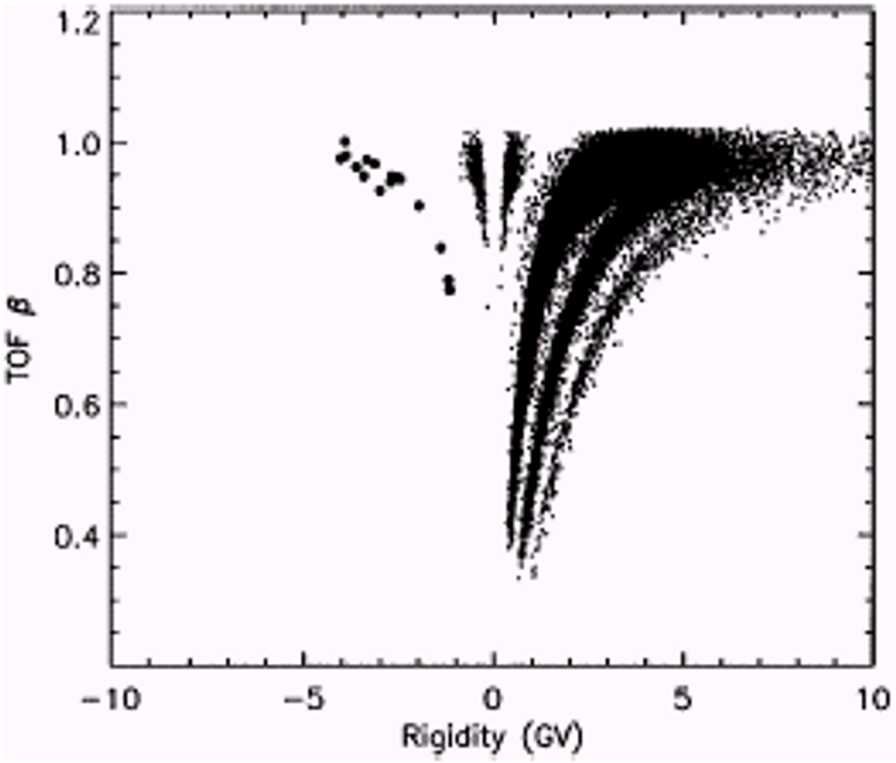

FIG. 1. Velocity determined by the TOF vs rigidity for events with C2 + C3 ≤ 0.36. The 16 antiprotons have been enhanced (●). Protons, deuterium, and tritium are visible at positive rigidity. The protons and antiprotons are clearly separated from the pions, muons, and electrons.

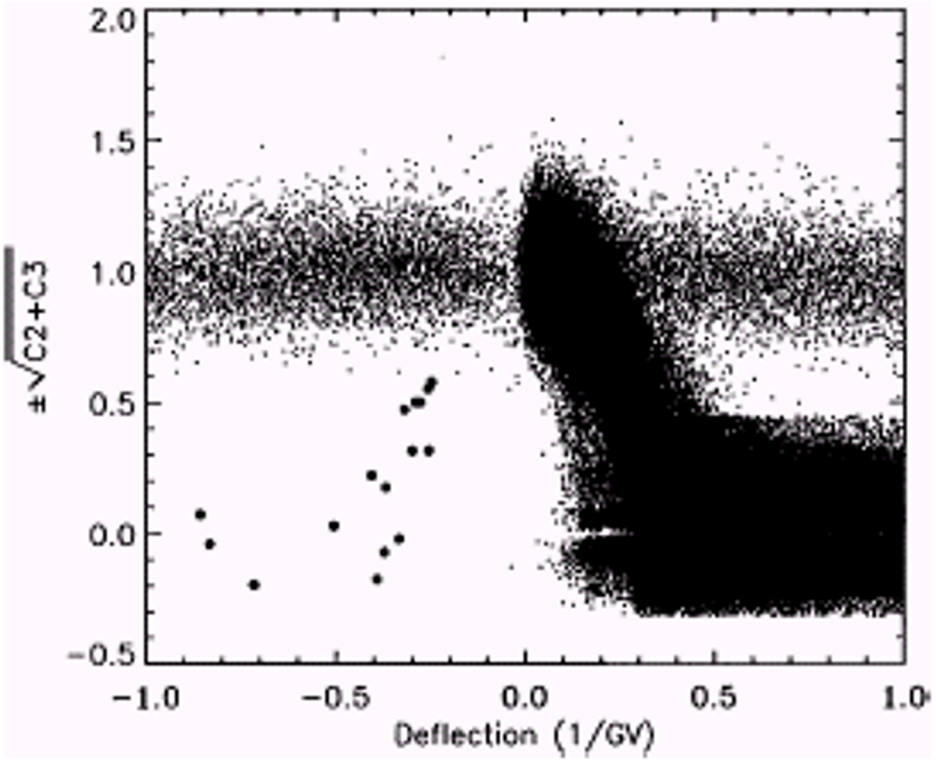

FIG. 2. The signed square root of the absolute value of the C2 + C3 signal vs deflection (proportional to rigidity^{-1}). The 16 antiprotons have been enhanced (●). Low-mass particles occupy the nearly horizontal band. The Cherenkov counter noise of ~0.5 photoelectron can result in negative values. At low amplitude, fluctuations in the signal are exaggerated by the square root. Below 3.2 GeV (0.6 ordinate) the antiprotons are well separated from background.

HEAT - The Transition Radiation Detector

A schematic cross-sectional view of the different detectors making up HEAT, in the first configuration for detection of electrons and positrons.

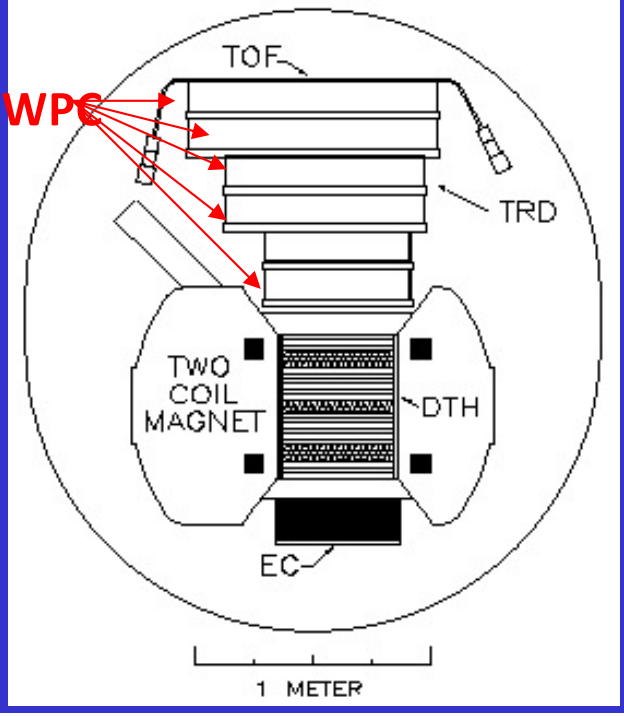

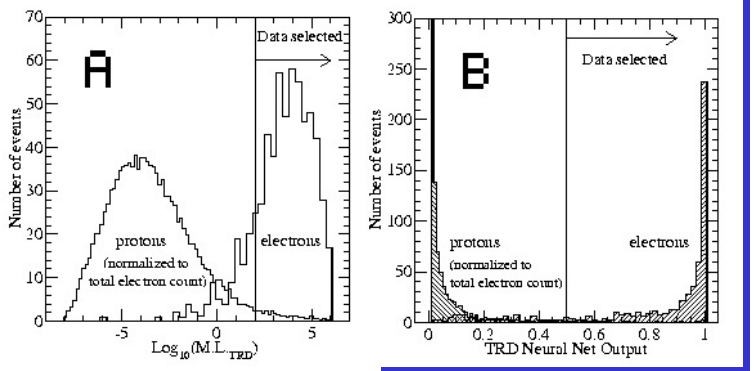

The HEAT Transition Radiation Detector

The Transition Radiation Detector (built by the University of Chicago) consists of six polyethylene fiber radiator blankets, each with a multi-wire proportional chamber MWPC (filled with a Xenon-methane gas mixture) attached underneath. When a charged particle travels through an interface between materials of different dielectric constants, radiation (in the form of X-rays) is generated with an intensity proportional to the relativistic Lorentz factor gamma of the particle. As it travels through a polyethylene fiber blanket, a high-energy electron (of high Lorentz gamma) encounters many interfaces and generates transition radiation, whereas a proton of the same energy (but a much lower Lorentz factor due to a higher mass) generates essentially no such radiation.

X-ray photons are absorbed by the gas mixture in the MWPC. The combination of energy deposited by the X-rays and ionization losses (due to the passage of any charged particle - electron or proton - through the gas in the chambers) is picked up electrically by cathode electrodes running perpendicular to the wires in the chamber (used in the pulse-height analysis below). Additionally, an electrical signal is also picked up by the wires in the chamber, and both a signal amplitude and variation with time are recorded (used in the time slice analysis below).

Pulse-height likelihood analysis

The total energy deposited in each of the six MWPCs is compared to the known signals (from prior calibrations) obtained when an electron, proton or alpha particle traverses the detector. A parameter is then calculated that indicates the likelihood that the particle was an electron (technically, the parameter is the product for all six chambers of the probability that the signal was produced by an electron or positron divided by the probability that the signal was produced by a proton). Figure A below shows the distribution of this maximum-likelihood parameter with clearly separated proton and electron populations.

Time slice analysis

A software neural-net classifier (with 3 input nodes, 5 hidden nodes and one output node) was devised, and trained to recognize the difference in the resulting time distribution of charge clusters detected by the wires when an electron or a proton traverses the detector. The output of the neural net analysis is a number between 0 and 1, indicating the probability that the particle was a proton (near 0) or an electron or positron (near 1). The excellent separation between protons and electrons is illustrated in figure B below.

HEAT: the T.O.F. system

The HEAT Time-of-Flight system

The Time-of-Flight system consists of four paddles of plastic scintillator viewed by eight photomultiplier tubes (built by the University of California at Berkeley), at the top of the instrument, and three paddles of scintillator viewed by three photomultiplier tubes (built by the University of California at Irvine), near the bottom of the instrument. **When a charged particle traverses a scintillator slab, a small amount of light (proportional to the square of the charge of the particle but inversely proportional to the square of its velocity) is generated; this light is viewed by the photomultipler tubes and converted to electrical pulses, that are then processed by assorted electronics module.**

Particle velocity and direction of travel

The accurate times at which light is seen at the top and bottom are recorded, and the time difference is used to calculate the velocity of the particle (expressed in units of the speed of light). We are especially interested in **discriminating** between **particles traveling downwards** through our instrument **and** the so-called albedo **particles traveling upwards** **(since an upgoing negatively charged particle could fool us into thinking it was a positively charged particle traveling downwards...).** That we have achieved excellent separation between upward and downward-going particles can be seen from figure A below (where by definition positive velocities represent downgoing particles and negative velocities upgoing).

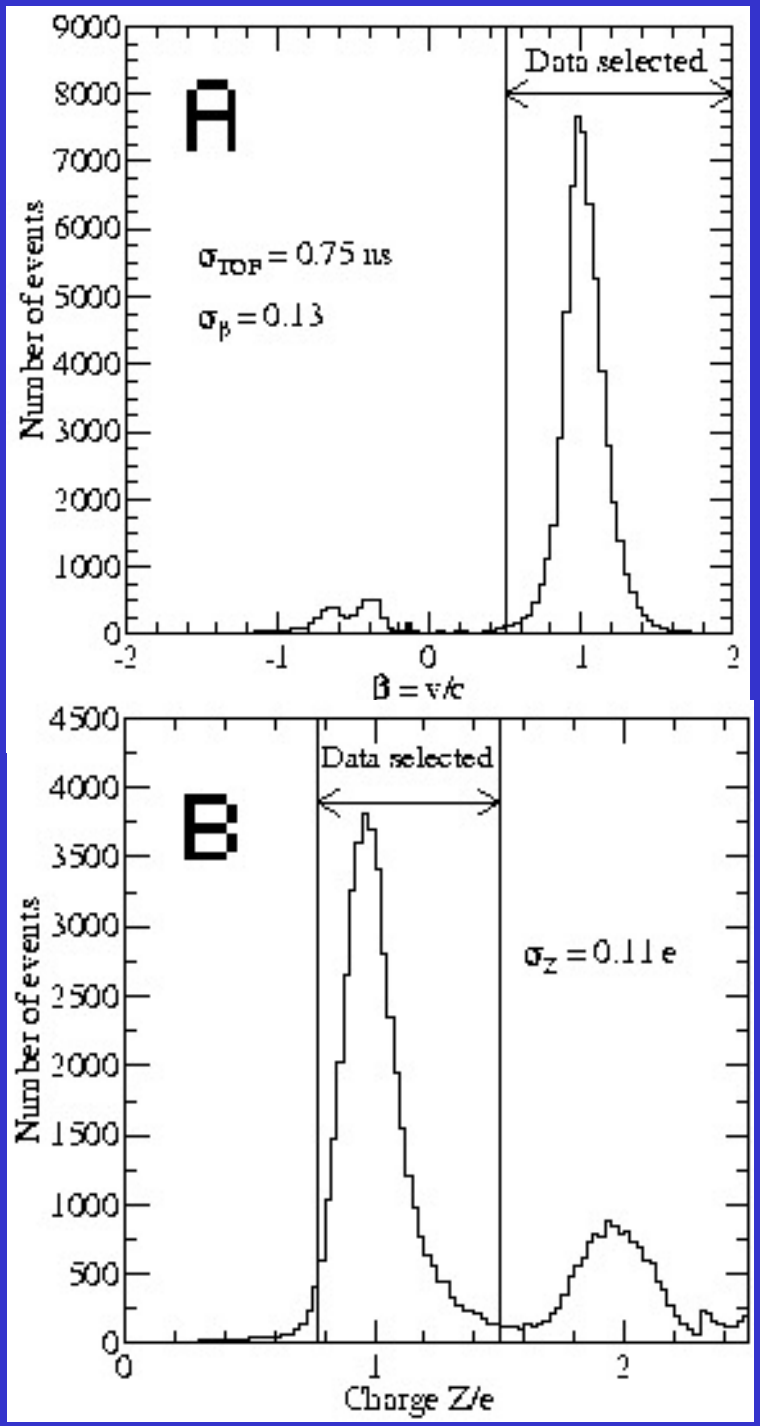

HEAT: the magnetic spectrometer

The Magnetic Spectrometer consists of two parts:

A magnet consisting of two superconducting coils inside a cryogenic vessel filled with liquid Helium, generating a magnetic field of 1 Tesla over a central room-temperature bore of dimensions 51 cm x 51 cm x 61 cm.

A precision tracking Drift-Tube Hodoscope, a chamber with 479 thin-walled drift tubes filled with a CO2-hexane gas mixture, arrayed in 26 layers (18 aligned parallel with the magnetic field, 8 perpendicular), located inside the bore of the magnet.

When an electrically charged particle travels through the magnetic field permeating the hodoscope, its trajectory is deflected due to the Lorentz force, in a direction perpendicular to the magnetic field. As the particle travels through the gas inside the tubes, it deposits an electrical signal picked up by a thin wire running down the center of the tube, and from the time at which the signal was picked up in the various tubes, it can be determined to high accuracy (about

70 microns) how far from the wire the particle was traveling. We thus obtain a pattern of lined-up "impact parameters" (distance of closest approach), as illustrated in the figure below (black circles inside the gray tubes; the red tubes were rejected in this event although they had fired).

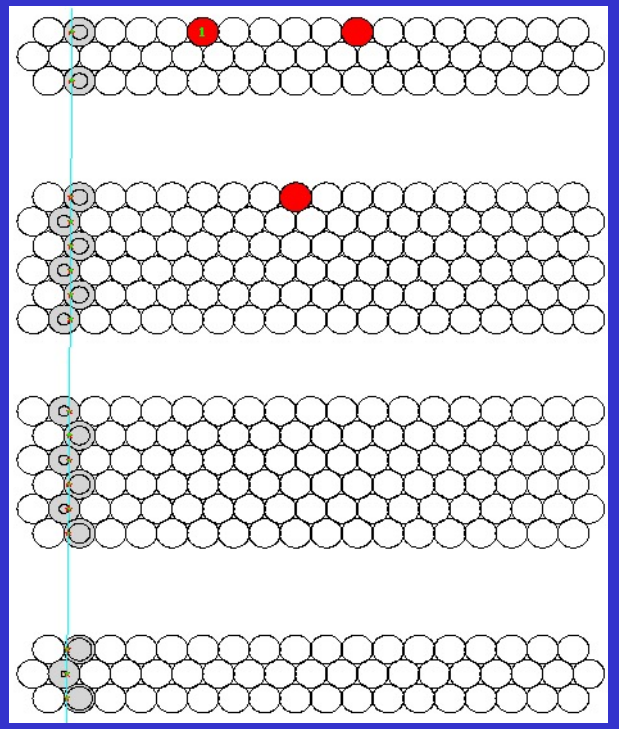

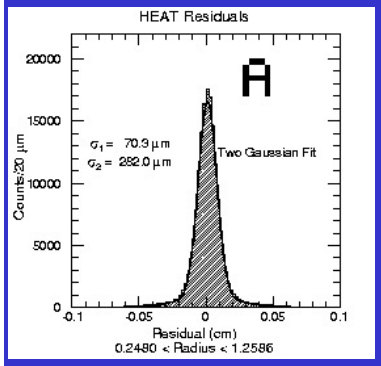

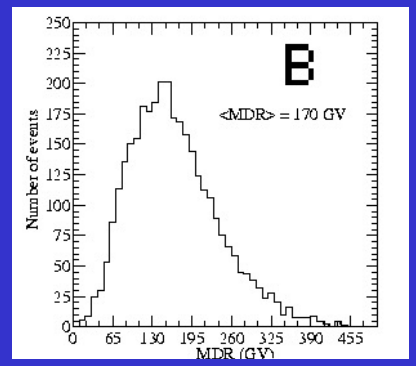

HEAT - The electromagnetic calorimeter

The Electromagnetic Calorimeter (built by the University of California at Irvine) consists of ten plastic scintillator slabs viewed by one photomultiplier tube each, interspersed with ten layers of Lead (each of a thickness equivalent to 0.9 electron radiation length), located at the bottom of the instrument. When an electron or a hadron reaches the Lead layers, a shower of secondary particles is produced and propagates through the rest of the stack (most of the secondary particles themselves produce further showering in deeper Lead layers), until the energy of the parent particle is expended and the particle shower is eventually absorbed. When charged particles traverse the scintillator slabs, light is generated and detected by the photomultipler tubes (and then converted to electrical pulses, processed by assorted electronics module), in amounts proportional to the number of particles in the scintillator.

Shower shape discrimination

By measuring the number of particles in the shower at each scintillator layer in the stack (the so-called shower profile), we can distinguish between showers initiated by electrons or positrons from those initiated by hadrons

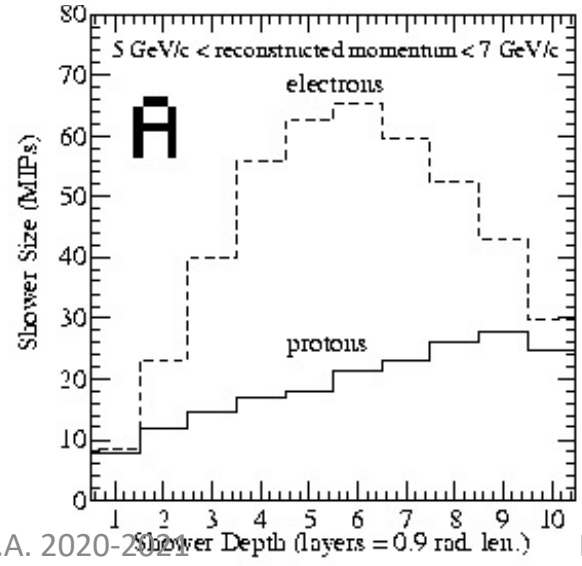

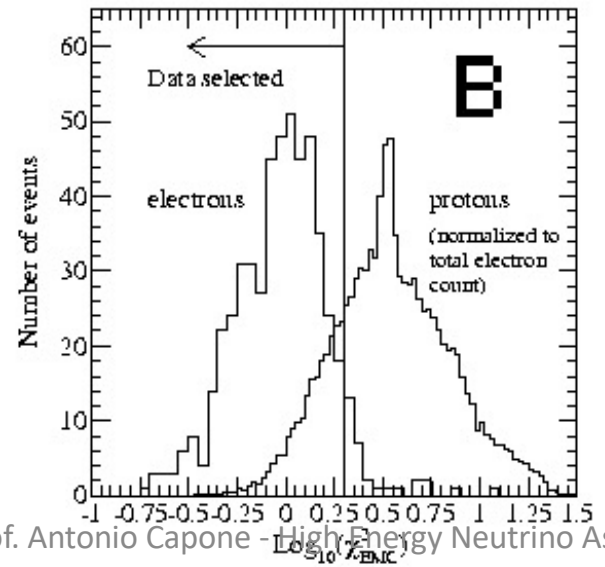

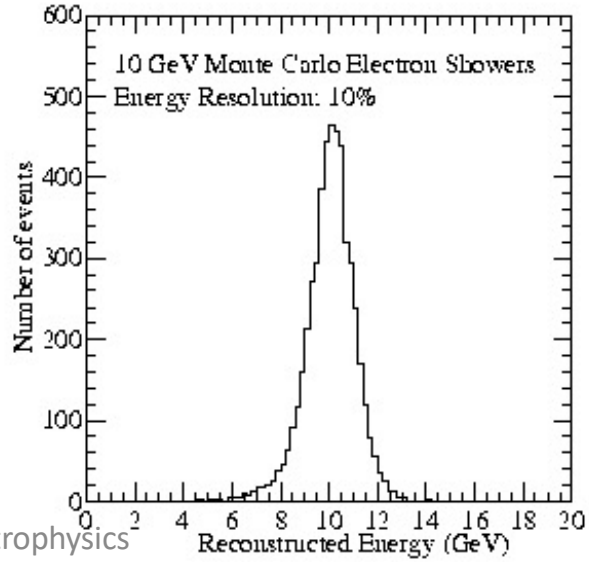

BESS - Balloon Superconducting Solenoid Experiment

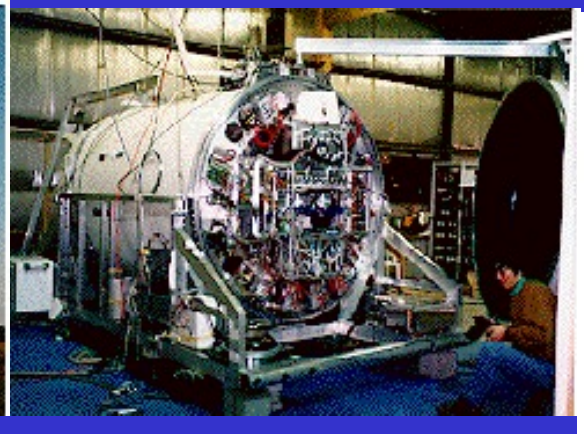

Primary scientific objectives of the experiment are the measurements of the cosmic antiproton energy spectrum, very sensitive search for antihelium, and the precision measurements of various cosmic ray components.

The BESS detector has a unique cylindrical configuration with a large acceptance of 0.4, which is one order of magnitude larger than that of previous spectrometers.

Forty low energy cosmic antiprotons were clearly detected for the first time by the BESS detector.

Anti-helium

BESS experiment already has placed an upper limit on anti-helium to helium ratio of 2×10^{-6}, which is a factor improvement over previous experiments, which is a factor of 50 improvement over previous experiments.

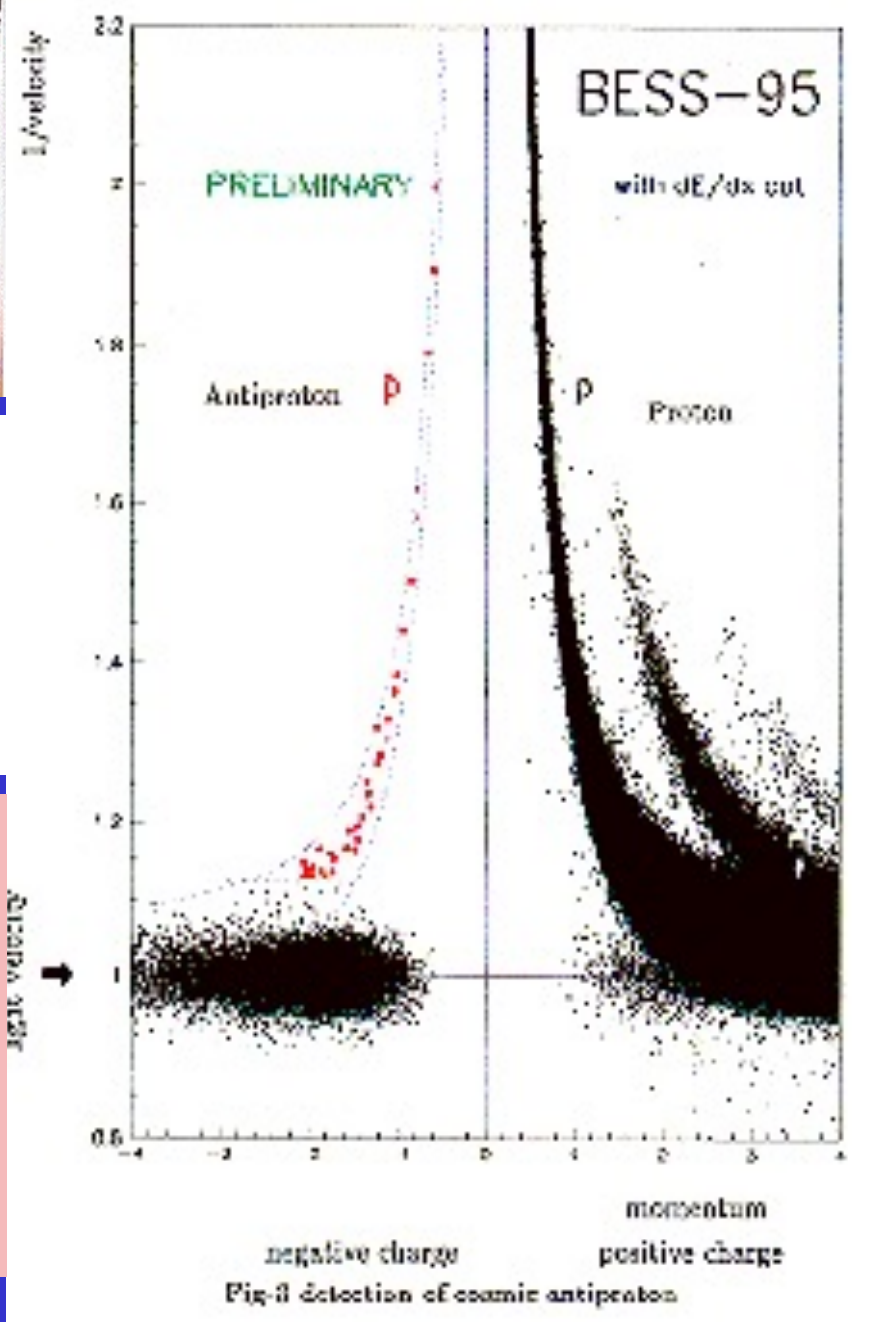

Fig-3 detection of cosmic antiproton

Proton/antiproton ratio

In 79 Golden et al. they observed antiprotons in cosmic rays. Sign of a symmetrical universe for matter and antimatter ???.

Expected antiprotons in C.R. interactions (protons, He +, heavier nuclei, ...) with interstellar matter (ISM).
The comparison between expected and measured fluxes can offer data to "model" the transport of R.C. (particularly the heaviest nuclei) in the ISM.

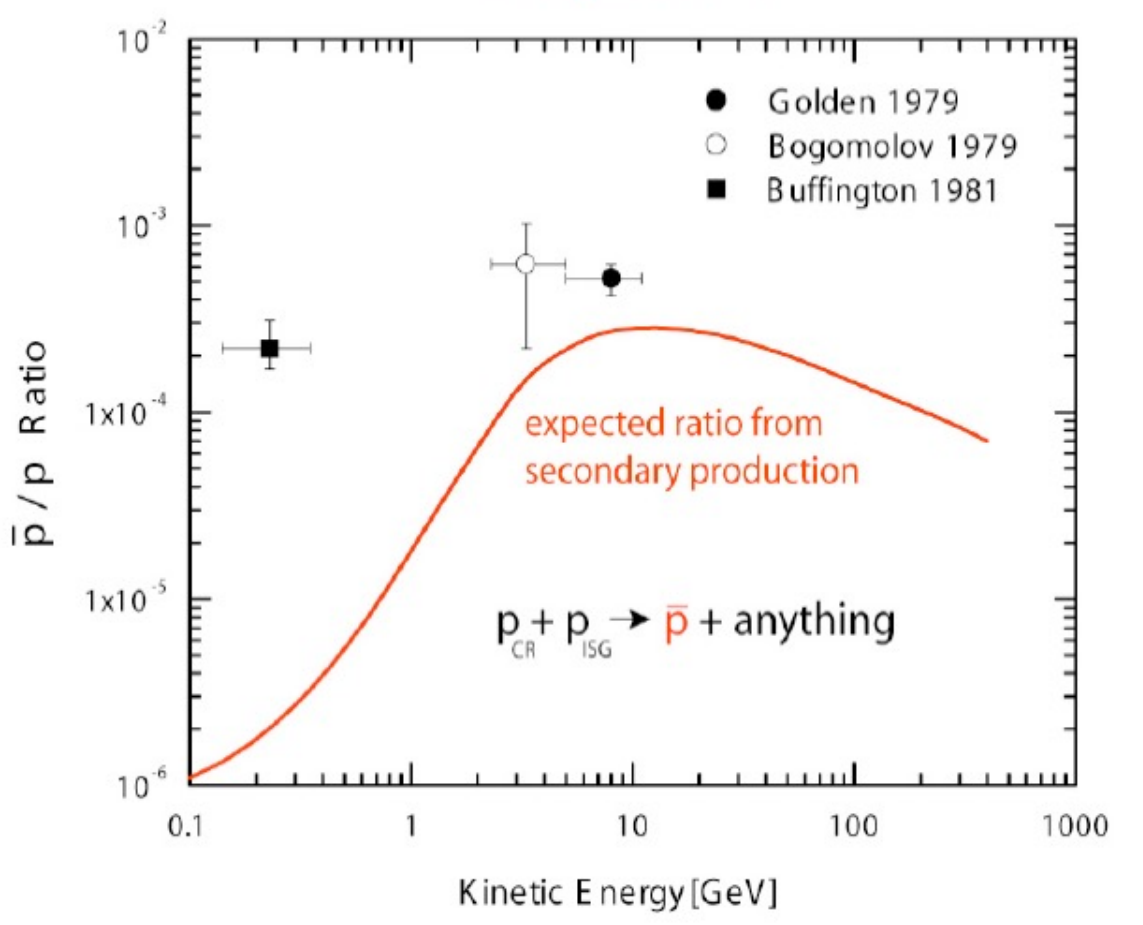

Other "exotic" sources have also been considered, such as "evaporation of primordial black holes, decay of "dark matter", acceleration in relativistic plasma, ...
The measures of BESS, MASS2, IMAX, and CAPRICE are in agreement with the model that the majority of antiprotons are secondary products of the interaction of R.C. primary

The Observatory PAMELA
2006 - 2016

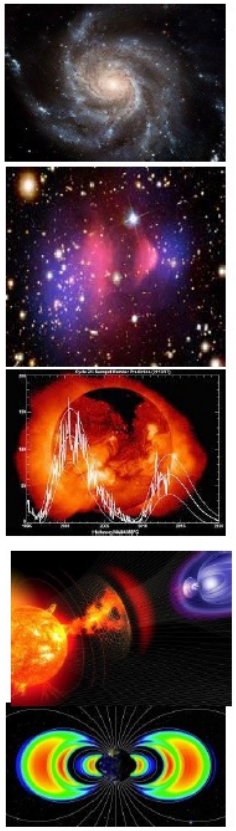

Precise measurements of protons, electrons, their antiparticles and light nuclei in the cosmic radiation

- Search for Dark Matter indirect signatures
- Search for antihelium (primordial antimatter) and new form of matter in the Universe (Strangelets?)
- Investigation of the cosmic-ray origin and propagation mechanisms in the Galaxy, the heliosphere and the terrestrial magnetosphere
- Detailed measurement of the high energy particle populations (galactic, solar, geomagnetically trapped and albedo) in the near-Earth radiation environment

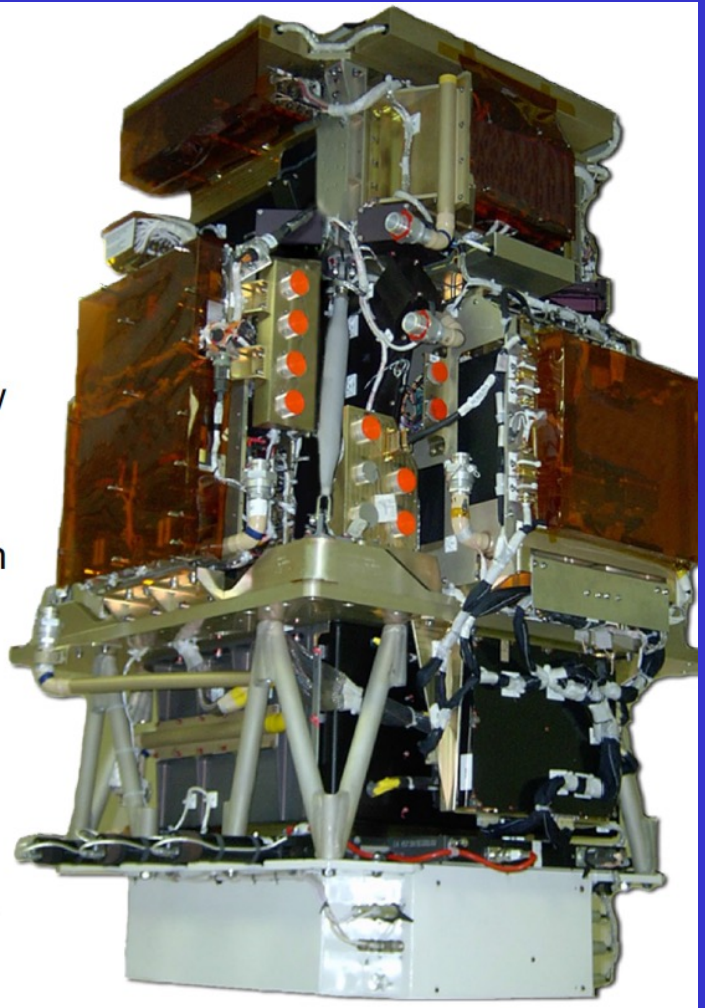

Payload for **A**ntimatter **M**atter **E**xploration and **L**ight-nuclei **A**strophysics

The PAMELA Instrument

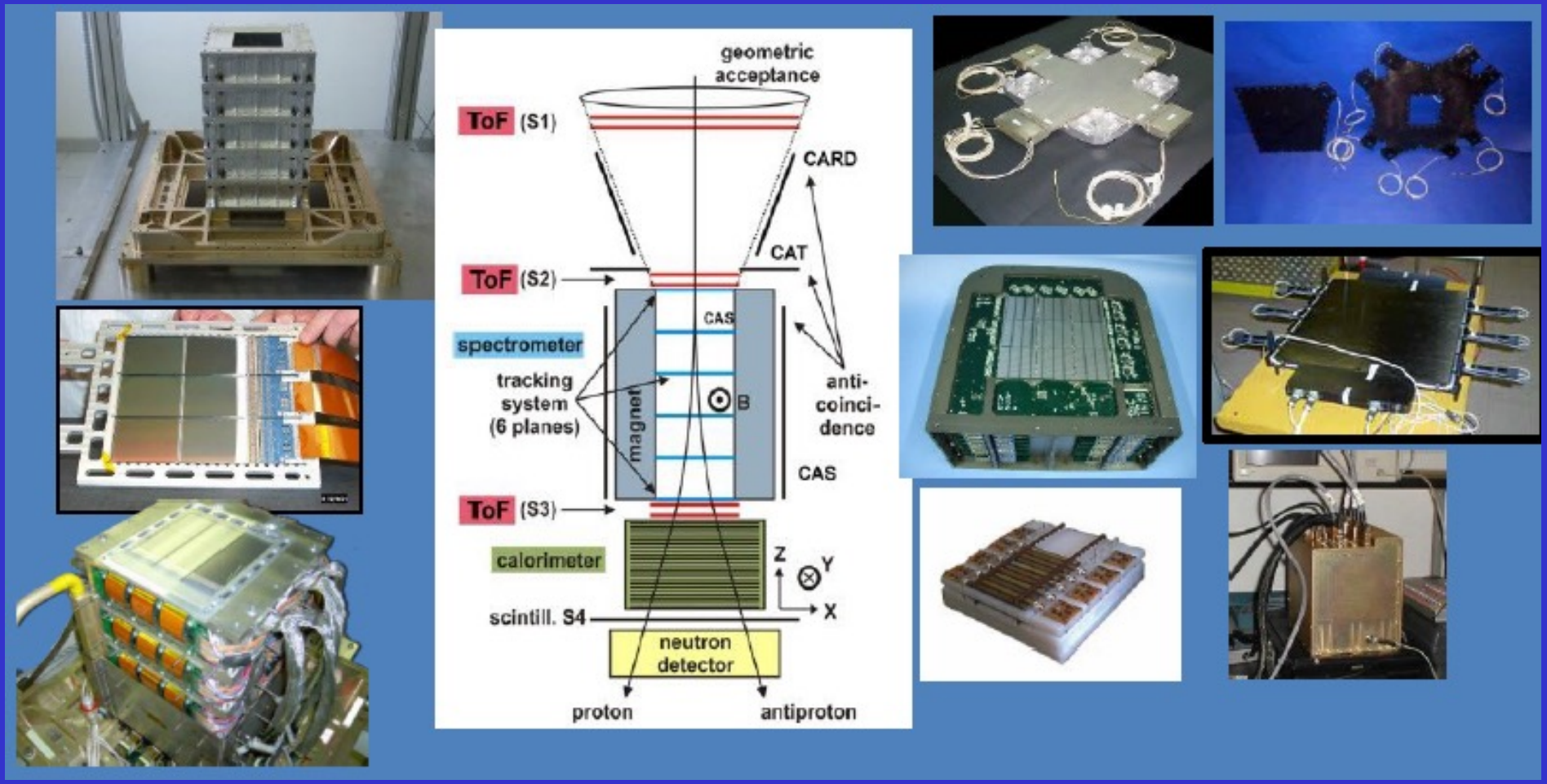

PAMELA results: positrons

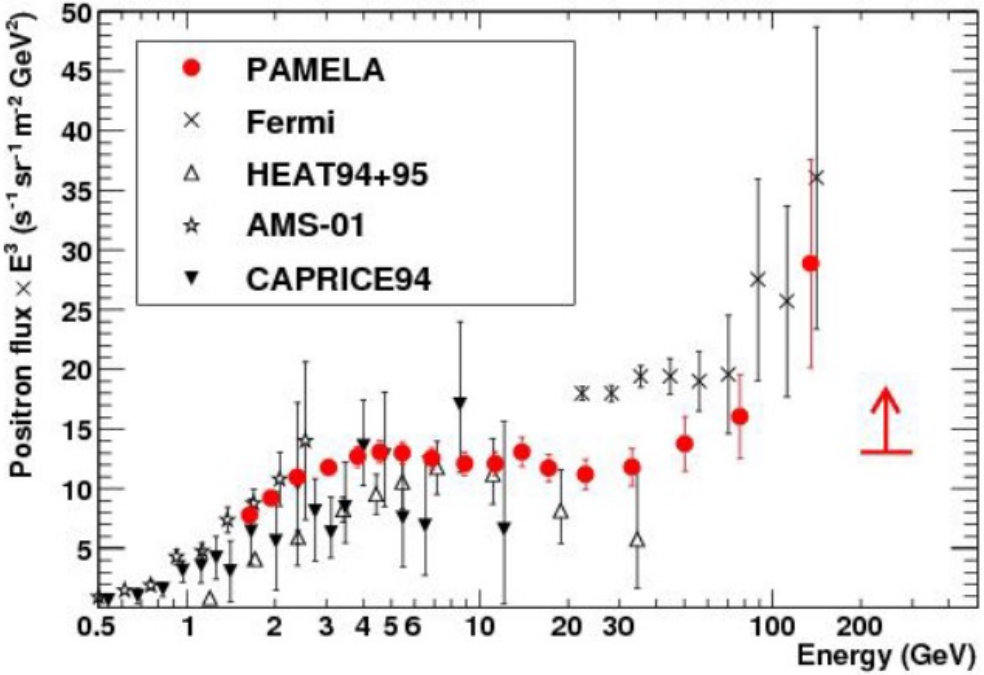

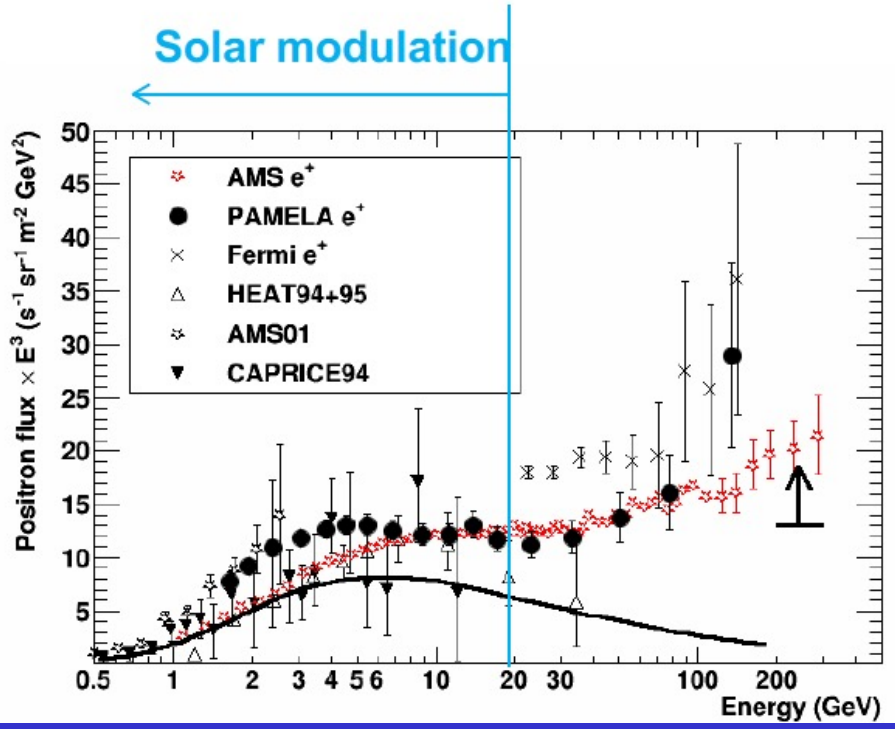

Pamela positron fraction

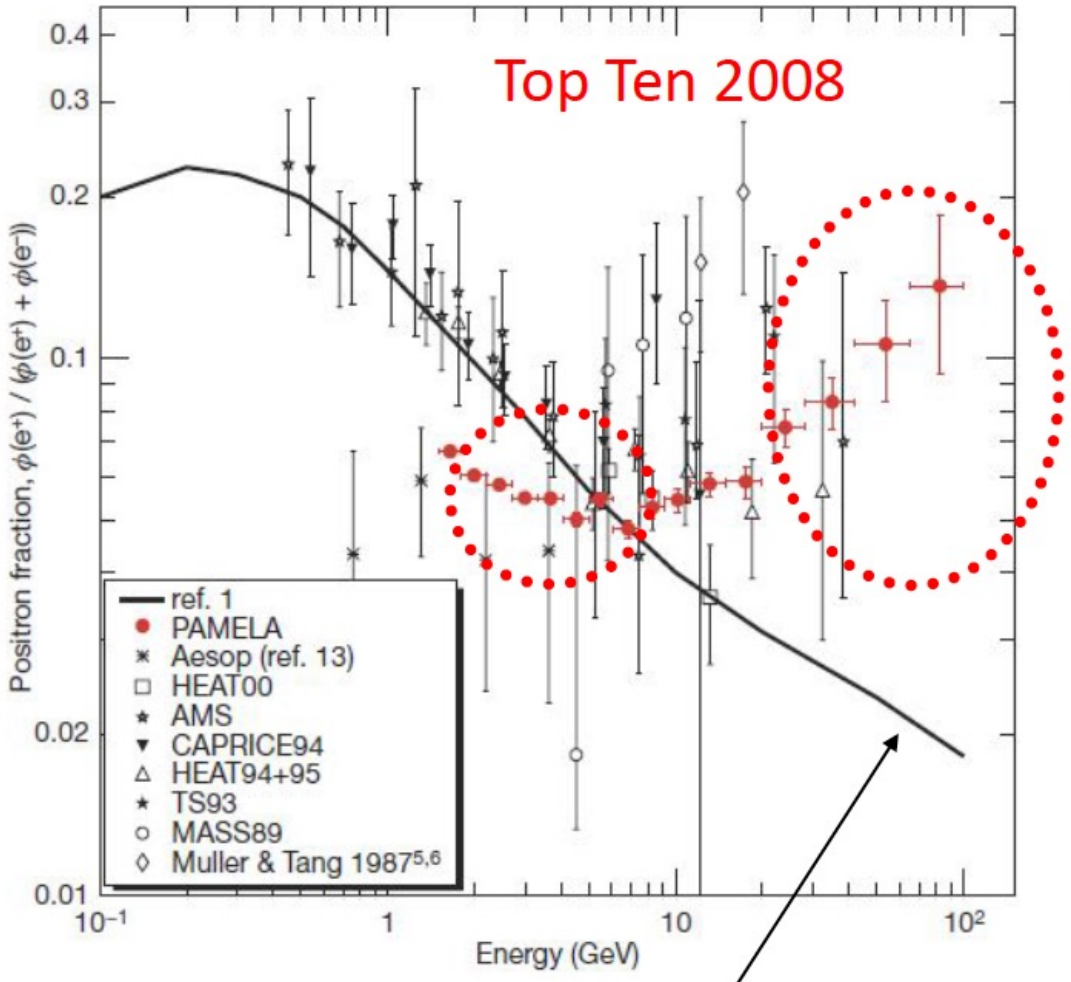

Secondary production: Moskalenko & Strong 98

nature International weekly journal of science

An anomalous positron abundance in cosmic rays with energies 1.5–100 GeV

O. Adriani[1,2], G. C. Barbarino[3,4], G. A. Bazilevskaya[5], R. Bellotti[6,7], M. Boezio[8], E. A. Bogomolov[9], L. Bonechi[1,2], M. Bongi[2], V. Bonvicini[8], S. Bottai[2], A. Bruno[6,7], F. Cafagna[7], D. Campana[4], P. Carlson[10], M. Casolino[11], G. Castellini[12], M. P. De Pascale[11,13], G. De Rosa[4], N. De Simone[11,13], V. Di Felice[11,13], A. M. Galper[14], L. Grishantseva[14], P. Hofverberg[10], S. V. Koldashov[14], S. Y. Krutkov[9], A. N. Kvashnin[5], A. Leonov[14], V. Malvezzi[11], L. Marcelli[11], W. Menn[15], V. V. Mikhailov[14], E. Mocchiutti[8], S. Orsi[10,11], G. Osteria[4], P. Papini[2], M. Pearce[16], P. Picozza[11,13], M. Ricci[17], S. B. Ricciarini[2], M. Simon[15], R. Sparvoli[11,13], P. Spillantini[1,2], Y. I. Stozhkov[5], A. Vacchi[8], E. Vannuccini[2], G. Vasilyev[9], S. A. Voronov[14], Y. T. Yurkin[14], G. Zampa[8], N. Zampa[8] & V. G. Zverev[14]

April 2nd, 2009

Citations: >1340

- High energy: first clear evidence of increasing positron fraction above 10 GeV with respect to pure secondary production;
- Low energy: charge-dependent solar modulation

PAMELA results: antiprotons

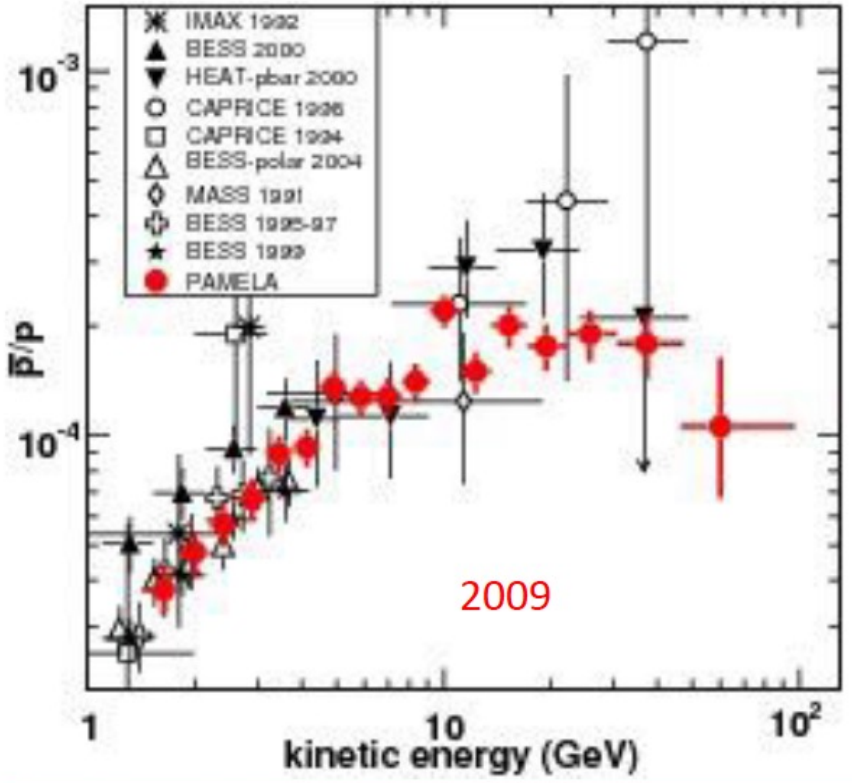

PHYSICAL REVIEW LETTERS

Highlights Recent Accepted Collections Authors Referees Search Press About

Featured in Physics Editors' Suggestion

New Measurement of the Antiproton-to-Proton Flux Ratio up to 100 GeV in the Cosmic Radiation

O. Adriani *et al.* (PAMELA Collaboration)
Phys. Rev. Lett. **102**, 051101 – Published 2 February 2009

Physics See Viewpoint: Debating the source of a rare particle

PHYSICAL REVIEW LETTERS

Highlights Recent Accepted Collections Authors Referees Search Press About

Featured in Physics Editors' Suggestion

PAMELA Results on the Cosmic-Ray Antiproton Flux from 60 MeV to 180 GeV in Kinetic Energy

O. Adriani *et al.*
Phys. Rev. Lett. **105**, 121101 – Published 13 September 2010

Physics See Synopsis: Uncertain sources

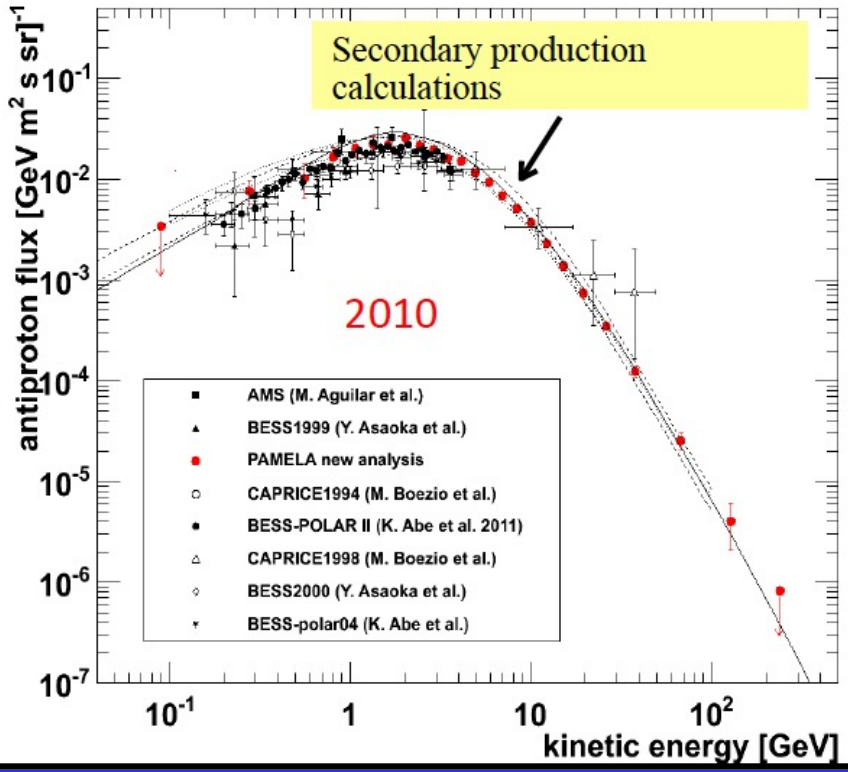

PAMELA Results possible explanations

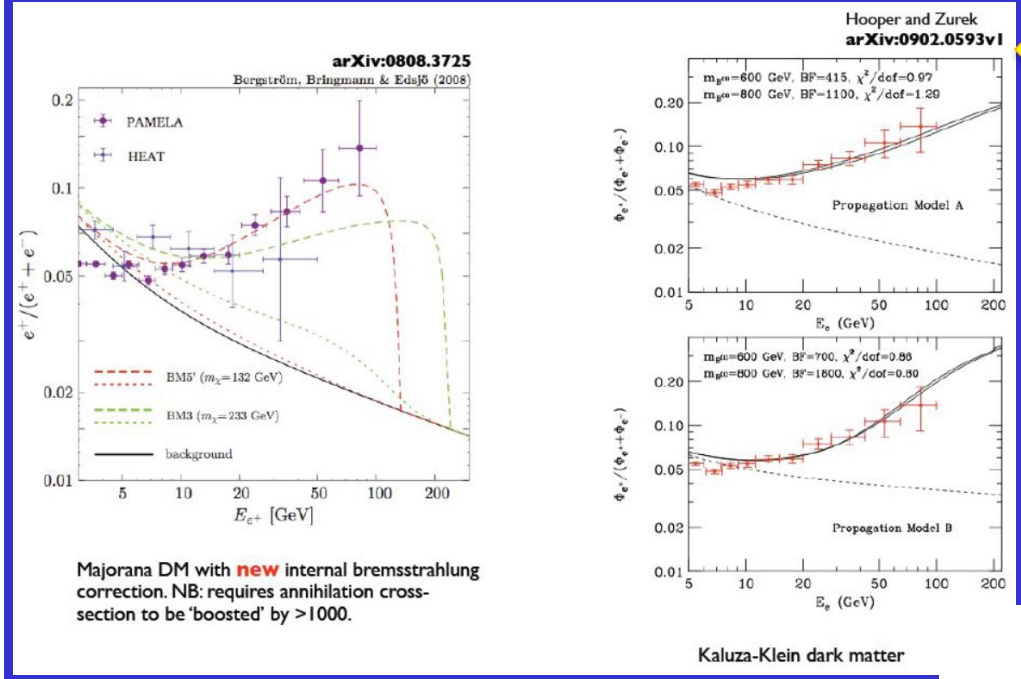

Majorana DM with **new** internal bremsstrahlung correction. NB: requires annihilation cross-section to be 'boosted' by >1000.

Kaluza-Klein dark matter

Dark Matter particles annihilate and from the "vacuum" → $e^+ e^-$

A "local pulsar": the spinning B of the pulsar strips e^- that accelerated emit γ that originate $e^+ e^-$

PULSAR → e^- → γ → $e^+ e^-$

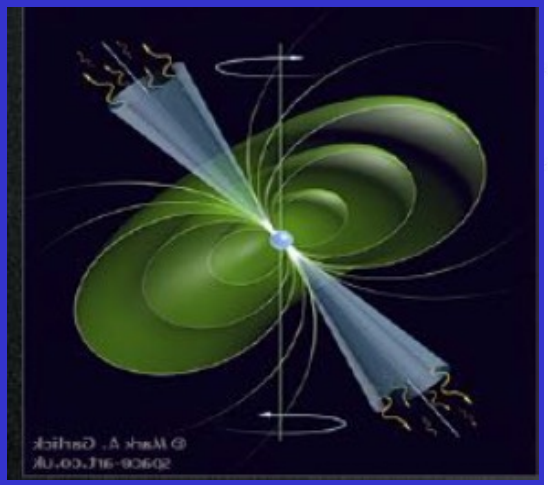

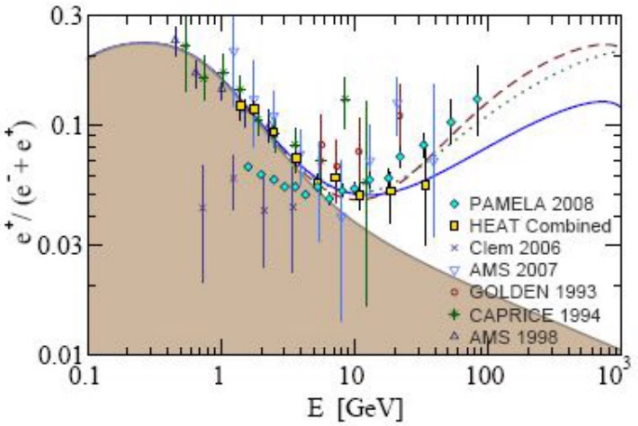

H. Yüksak et al., arXiv:0810.2784v2
Contributions of e- & e+ from Geminga assuming different distance, age and energetic of the pulsar

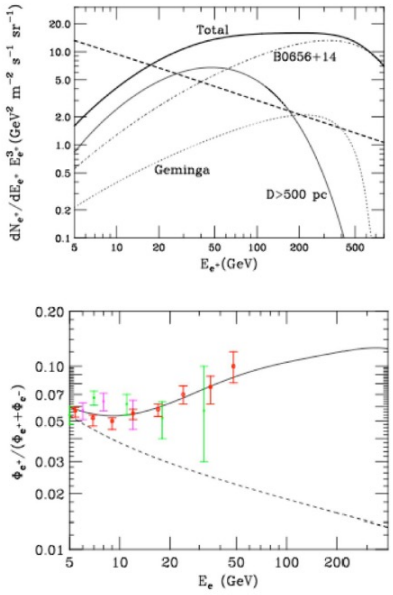

Hooper, Blasi, and Serpico
arXiv:0810.1527

PAMELA, other results: the B and C fluxes

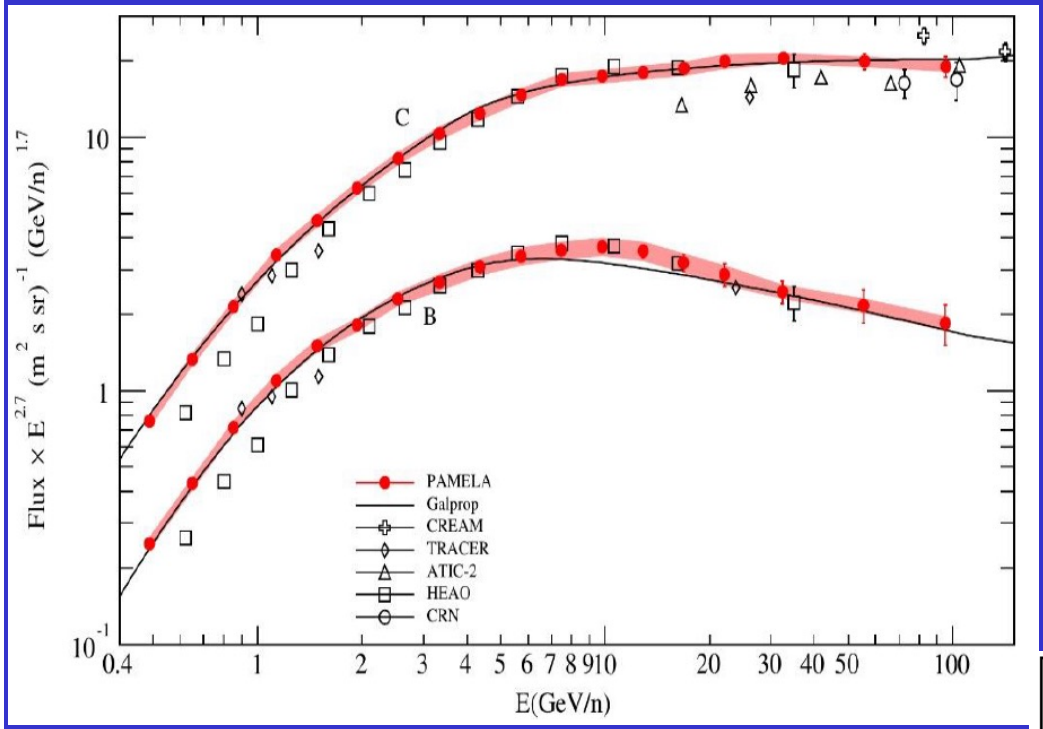

O. Adriani et al. ApJ 791 (2014), 93

B/C = Sec/Prim

~ $Q_{sec}(E)/Q_{prim}(E)$

~ $Q_{prim}(E)/D(E)$ / $Q_{prim}(E)$

~ $1/D(E)$

Diffusion coefficient: $D(R)=D_0\beta R^{\delta}$

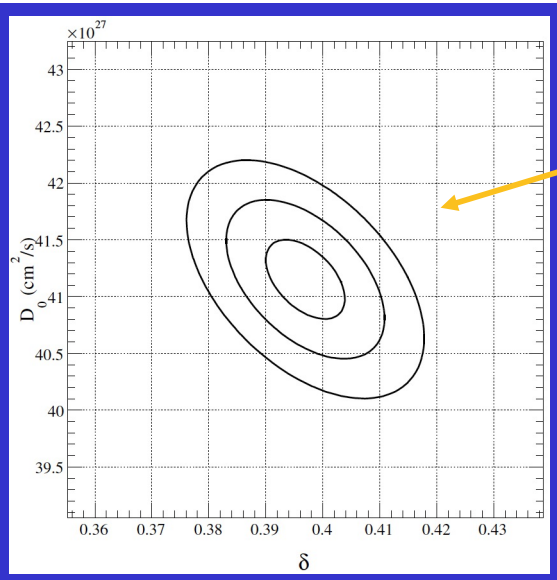

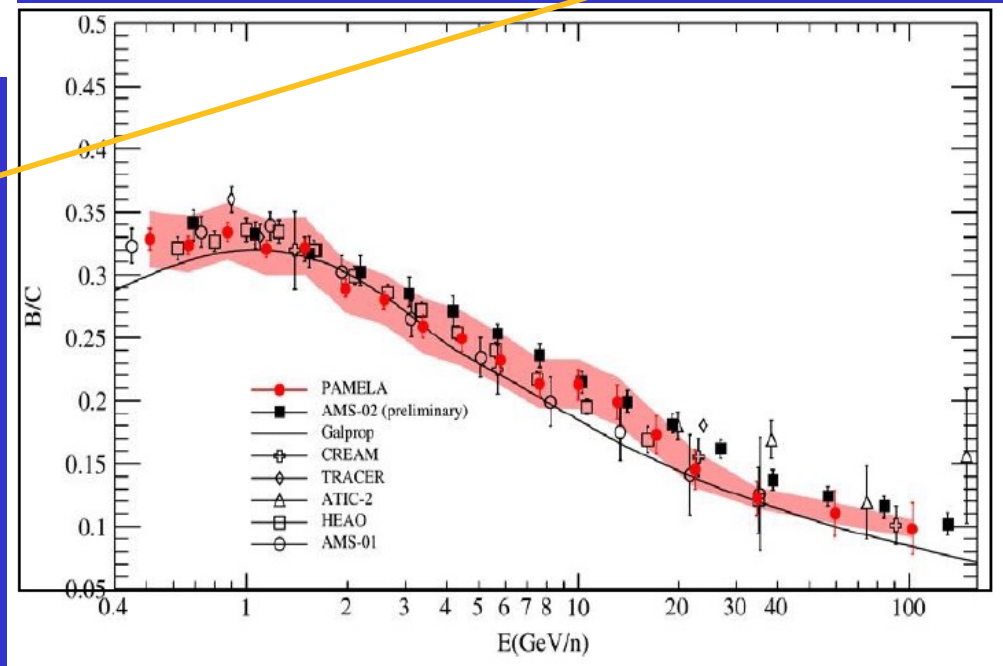

PAMELA overall results

Physics Reports
Volume 544, Issue 4, 30 November 2014, Pages 323–370
The PAMELA Mission: Heralding a new era in precision cosmic ray physics

The PAMELA Mission: Heralding a new era in precision cosmic ray physics

- Results span 4 decades in energy and 13 in fluxes
- The PAMELA collaboration published more than 80 papers on international journals such as: Nature, Science, Physics Reports, Physical Review Letters, Astrophysical Journal, etc..

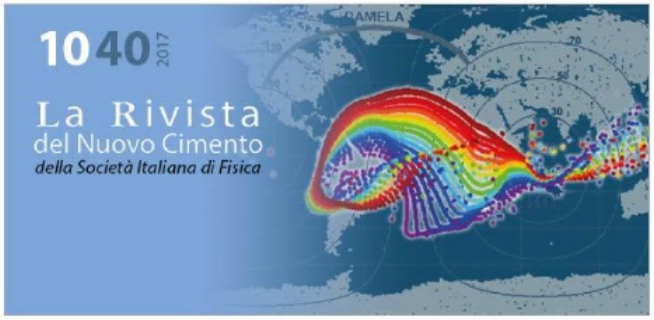

TEN YEARS OF COSMIC RAYS IN SPACE

A new issue of La Rivista del Nuovo Cimento on the role of a satellite-borne detector uncovering the mysteries of cosmic rays

La Rivista del Nuovo Cimento Vol. 40 N. 10: online in OPEN ACCESS for 30 days

Ten years of PAMELA in space

PAMELA Collaboration

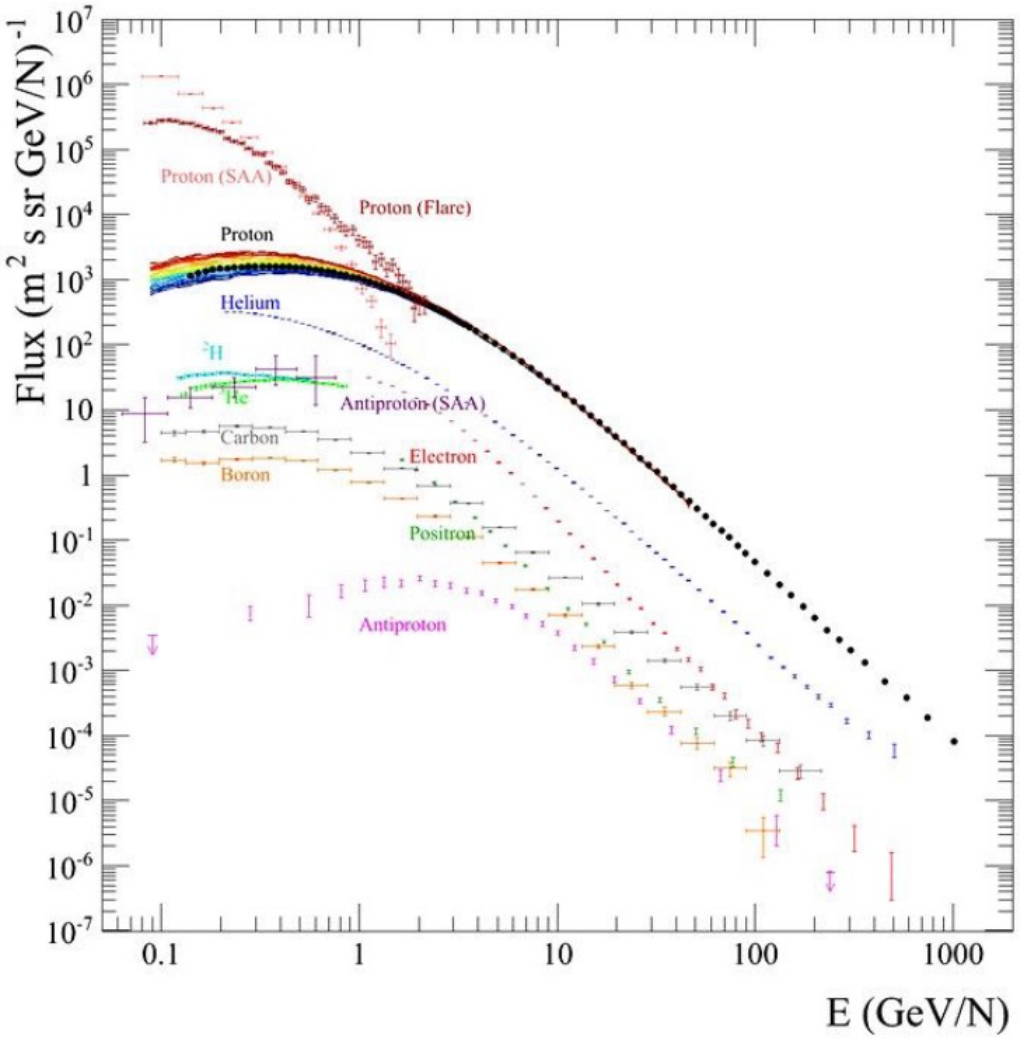

INTErnational Gamma-Ray Astrophysics Laboratory